

Normalized Cut with Adaptive Similarity and Spatial Regularization *

Faqlang Wang [†], Cuicui Zhao [†], Jun Liu [†], Haiyang Huang [†]

Abstract

In this paper, we propose a normalized cut segmentation algorithm with spatial regularization priority and adaptive similarity matrix. We integrate the well-known expectation-maximum(EM) method in statistics and the regularization technique in partial differential equation (PDE) method into normalized cut (Ncut). The introduced EM technique makes our method can adaptively update the similarity matrix, which can help us to get a better classification criterion than the classical Ncut method. While the regularization priority can guarantee the proposed algorithm has a robust performance under noise. To unify the three totally different methods including EM, spatial regularization, and spectral graph clustering, we built a variational framework to combine them and get a general normalized cut segmentation algorithm. The well-defined theory of the proposed model is also given in the paper. Compared with some existing spectral clustering methods such as the traditional Ncut algorithm and the variational based Chan-Vese model, the numerical experiments show that our methods can achieve promising segmentation performance.

Keywords: Normalized cut, Spectral Clustering, EM Algorithm, Operator Splitting, TV.

1 Introduction

Image segmentation is an important and attractive field in image processing, which plays an important role in many applications. The goal of image segmentation is to obtain a meaningful partition for an image to do some further tasks, including feature extraction, image classification and object recognition. In general, the segmentation result of an image is some partitions which cover the whole image, or some contours that separate the image into different regions, such that the pixels in the same region share some similarities such as intensity, texture and color.

A great deal of the segmentation models have been proposed in the literature. In which the edge based segmentation methods such as snakes and active contour models [21, 6] are popular research branch in image segmentation. Another segmentation method is the Markov Random Field [30] and expectation maximum (EM) [4] based statistical methods [22]. In such a method, pixels are often regarded as some samples taken from a random variable whose distribution is a parametrical mixture model. Besides, clustering based methods treat pixels as data points and convert image segmentation to a clustering process, such as K-means based methods [20, 7] and spectral clustering based methods [31, 37]. In addition, learning-based segmentation methods draw much attention recently, especially for the deep learning neural network based methods. Usually, the learning based methods need a large amount of labeled data to train some desirable networks [11, 19, 42, 13]. To be different from learning based method, variational approaches can obtain a segmentation from a single image by minimizing a cost functional which consists

*This work was supported by The National Key Research and Development Program of China (2017YFA0604903).

[†]Laboratory of Mathematics and Complex Systems (Ministry of Education of China), School of Mathematical Sciences, Beijing Normal University, Beijing, 100875, People's Republic of China. Jun Liu: jliu@bnu.edu.cn .

of the data and regularization terms. Here the data term is a clustering criterion, and the regularization term usually contains some prior information of segmentations. For examples, one can use the well-know total variation (TV) to punish the length of region contour [7, 25], and to get some smooth segmentation boundaries. In order to get some special geometrical shape, star shape prior regularization [35] and convexity constraint regularization term [17, 24] can be adopted. Meanwhile, the regularization technique can improve the precision of segmentation and enhance the robustness of the result under noise [2]. The variational methods and learning based methods both have promising performance. The main differences between these two methods are the supervised samples. The variational methods just need a single image without labels while learning based methods often need massive images with labels. In this paper, we pay more attention on the variational methods, which are flexible to combine many methods together.

Here we give some introductions for clustering based methods. A popular K-means based segmentation model is Chan-Vese (CV) model [7], which consists of K-means clustering data term and TV regularization. CV has a good segmentation performance for some linear separated data. However, the CV model partly depends on the initial values and tends to obtain a local minimum. Besides, CV model can not address the clustering problem of nonlinear separable data set, such as the nested double moons data set since the K-means is a linear boundary based clustering algorithm. Spectral clustering [36] is also a widely used clustering algorithm, the key idea of spectral clustering is to transfer the data points into an nonlinearly feature space, in which the data can be easily segmented by some simple linear clustering algorithms. In spectral graph theory [9], spectral clustering is equal to a min-cut problem, which can be solved by some global minimization algorithms, and they are independent of initial values.

Due to spectral clustering has much stronger nonlinear separable ability, numerous segmentation methods based on spectral clustering have been proposed. In these methods, an image is represented as an undirected weighted graph, in which the nodes correspond to the image pixels and the edges connect pairs of nodes equipped with weights measuring the similarity between nodes. Then the image segmentation is equivalent to finding a min-cut for such a graph. The work of Ulrike Von Luxburg [36] provides a comprehensive review of spectral clustering. Hagen and Kahng present a cheeger cut criterion based clustering method [18], which shows better performance. Shi and Malik establish a new balanced graph cut criteria: normalized cut (Ncut) [31], aiming at overcoming the drawbacks of traditional cut criteria based model [37]. Szlam and Bresson [32], Buhler and Hein [5] found the relationship between spectral clustering and nonlocal total variation [15], respectively, which provide spectral clustering theoretical supports. Since the normalized cut problem can be relaxed to an eigenvalue system, many normalized cut based models have been proposed. Yu and Shi [40] establish the Ncut model with linear homogeneous equality constraints. It is extended to the situation of non-homogenous equalities by Eriksson et al. [12]. Bernard et al. [14] proposed a new framework to solve the Ncut problem with priors and convex constraint by Dinkelbach method [29]. All the related works reveal that the segmentation method based on spectral clustering is well-behaved and has tremendous potential.

Though these mentioned spectral clustering based methods are proved having good performance, some flaws still exist. For instance, these methods are sensitive to noise which makes the methods unstable since they lack of spatial prior information. Moreover, one should give the similarity matrix in advance during the spectral clustering procedure, and the choice of parameters in the similarity matrix is intractable. Tang et al. [33] combines MRF regularization with normalized cut to show better robustness. However, the model adopts KNN affinity (similarity) construction in normalized cut procedure which is a bit crude. Yu et al. [41] equip an L_1 -regularized energy term in cut based formulation to promote sparse solutions, and the affinities similarity of [31, 1] were adopted in a piecewise flat embedding model. However, all these models have less consideration of the similarity design.

To solve the problems existing in segmentation model based on spectral clustering, in this work, we integrate the well-known expectation-maximum (EM) method [4] in statistics and the regularization technique in PDE into the normalized cut, while the introduction of EM technique which is based on histogram modeling endows normalized cut an adaptive similarity matrix, and the regularization will enhance the robustness of the result under noise. To obtain an adaptive similarity, inspired by Gaussian Mixture Model and EM method, we deduce a model based similarity which can be updated iteratively to help us get a better classification criterion. In fact, normalized cut is a linear method, which equals to solve an eigenvalue system after relaxation, and the regularization will enhance spatial smoothness of the spectrum vector in fact. To unify the three totally different methods, we built a variational framework to naturally combine them and get a general normalized cut segmentation algorithm.

The main contributions of this paper include: firstly, we built a new variational framework of the normalized cut which unifies three totally different methods: EM, regularization, and spectral graph clustering, which makes the results of normalized cut image segmentation method numerical stability and better performance. To the best of our knowledge, this is the first research to combine these three methods together; Secondly, we establish the well-defined theory of the existence of the minimizer for the proposed model. Thirdly, compared with some existing spectral clustering based methods and classical Chan-Vese model, the numerical experiments show that our algorithm can achieve desirable segmentation performance.

The rest of this paper is organized as follows: we review the related works in section 2, containing Chan-Vese model, normalized cut, Gaussian Mixture Model and EM algorithm as well. Two variational based normalized cut models with adaptive similarity and regularization: Normalized Cut with Adaptive Similarity and H^1 regularization (NCASH¹) model and Normalized Cut with Adaptive Similarity and TV regularization (NCASTV) model, are proposed in section 3. Meanwhile, we prove the existence of the minimizer of NCASTV model in this part. Section 4 gives the algorithms and the details in implementation. In section 5, we show the experimental results. We summarize our methods and make some conclusions in section 6.

2 Related Works

In this section, we introduce some related works. First of all, we review the Chan-Vese model [7] briefly, and then we introduce classical Ncut model [31]. Meanwhile, the similarity matrix in traditional Ncut is parametric, which affects the segmentation results greatly, and the choice of parameters is troublesome. To solve this problem, inspired by the Gaussian Mixture Model and EM algorithm, we construct a variational framework of which optimal solution can measure the similarity of intensity between image points adaptively. For these reasons, we review Gaussian Mixture Model and EM algorithm in the last part of this section.

2.1 Chan-Vese Model [7]

Let $I : \Omega \rightarrow \mathbb{R}$ be the image defined in an open bounded set $\Omega \subset \mathbb{R}^2$, Chan-Vese model [7] considers a piecewise constant approximation model used for two phase segmentation

$$E(\phi, c_1, c_2) = \lambda_1 \int_{\Omega} |I(x) - c_1|^2 H(\phi(x)) dx + \lambda_2 \int_{\Omega} |I(x) - c_2|^2 (1 - H(\phi(x))) dx + \int_{\Omega} |\nabla H(\phi(x))| dx.$$

where ϕ is the signed distance function and H is the Heaviside function, c_1, c_2 are two unknown constants, $\lambda_1 > 0, \lambda_2 > 0$ are fixed weights parameters.

In fact, Chan-Vese model consists of K-means based data term and TV regularization. The traditional method to solve Chan-Vese model is evolving the level-set function by gradient flow to obtain the segmentation results. Recently, there are many fast operator splitting algorithms [10, 8, 16, 38] to solve it.

2.2 Normalized Cut [31]

Normalized cut method represents an image as an undirected weighted similarity graph $G = \langle V, E, W \rangle$, and then image segmentation is equivalent to finding a min-cut in a graph. Here V is the set of pixels, E is the edges between pixels, and W is the weight matrix which measures the similarity between pixels (similarity matrix). Here the graph G is undirected, that is, the similarity weight matrix W is symmetric. More details can be found in [36]. In fact, the similarity matrix is parametric and the parameters will affect the results of the data clustering or segmentation process.

Graph-Cut: Graph $G = \langle V, E, W \rangle$ has a partition (A, B) , such that $A \cup B = V, A \cap B = \emptyset$. Then the cut value between A and B is defined as

$$cut(A, B) = \sum_{x \in A, y \in B} w(x, y),$$

where $x, y \in V, w(x, y)$ is the weight between point x and y .

The segmentation models based on min-cut criterion [37] have been demonstrated good performance on some natural images. However, as the authors noticed in their work, the above cut criteria favors cutting small sets of isolated nodes in the graph, which is not desirable in real applications. To overcome the bias existing in cut based model, Shi and Malik [31] present the well-known normalized cut

$$Ncut(A, B) = \frac{cut(A, B)}{assoc(A, V)} + \frac{cut(A, B)}{assoc(B, V)},$$

where

$$assoc(A, V) = \sum_{x \in A, y \in V} w(x, y).$$

The introduction of the measure of the “size” of each partition improves the performance of image segmentation, while avoiding the segmentation bias. However, the minimization of the normalized cut is NP-Hard [31]. Fortunately, the problem can be relaxed to be a generalized-eigenvalue problem below, which can be solvable by

$$(D - W)\mathbf{f} = \lambda D\mathbf{f}, \text{ s.t. } \mathbf{f}^T D \mathbf{1} = 0.$$

Here the relaxation function \mathbf{f} of a binary variable can be used to label the segmentation, and D is the degree matrix [36] which is a diagonal matrix with $D_{ii} = \sum_j W_{ij}$.

The minimization of the relaxation of normalized cut [3] can be expressed as

$$\min_{\substack{\mathbf{f}^T D \mathbf{f} = 1 \\ \mathbf{f}^T D \mathbf{1} = 0}} \mathbf{f}^T (D - W) \mathbf{f}. \quad (1)$$

Then, it is easy to get the pixel-by-pixel version of (1)

$$\min_{f \in \mathbb{F}} \left\{ \sum_{x \in V} \sum_{y \in V} w(x, y) (f(x) - f(y))^2 \right\},$$

where $\mathbb{F} = \{f : V \rightarrow \mathbb{R} \mid \sum_{x \in V} f(x) d(x) = 0, \sum_{x \in V} d(x) f(x)^2 = 1\}$.

It is easy to see that the min-Ncut problem can be transformed to an optimization problem, and the similarity matrix appeared in Ncut method is empirically given in advance, which is parametric. In the next part, we will review the ideas of Gaussian mixture model and EM algorithm, which is helpful to establish an adaptive similarity.

2.3 Gaussian Mixture Model and its Parameters Estimation

A Gaussian mixture model (GMM) can be expressed as

$$p(x; \Theta) = \sum_{j=1}^M a_j p_j(x; \theta_j),$$

where x is continuous-valued data vector, $\Theta = \{a_j, \theta_j\}$ is a set of parameters. And $\{a_j\}$ are the mixture weights, which satisfy the constraint that $\sum_{j=1}^M a_j = 1$, $p_j(x; \theta_j)$ are the j -th component Gaussian density functions, here $j = 1, \dots, M$.

Generally, the parameters of GMM are estimated by the iterative EM algorithm or maximum a posteriori (MAP) estimation from a well-trained prior model [28].

2.4 Expectation Maximum Algorithm

Expectation maximum (EM) algorithm is a classical method for parameters estimation of mixture models. It is used when the data has some missing values, or when optimizing the likelihood function is analytically intractable, but the likelihood function can be simplified by assuming the existence of some values [4]. EM algorithm has great applicability because of its stable convergence and convenient operation.

Assume N -dimension random variable $X = \{X_1, X_2, \dots, X_N\}$, and $p(\mathbf{x}; \Theta)$ is the density function of a gaussian mixture distribution governed by a set of parameters Θ . Given data set $\mathbf{x} = (x_1, x_2, \dots, x_N)$, by independent distribution assumption, one can get the log likelihood function of the parameters is

$$L(\Theta) = \ln(p(\mathbf{x}; \Theta)) = \ln\left(\prod_{i=1}^N p(x_i; \Theta)\right) = \sum_{i=1}^N \ln\left(\sum_{j=1}^M a_j p_j(x_i; \theta_j)\right),$$

which is difficult to optimize because it contains the log of the sum. However, if we consider X is incomplete, and assume that there is an unobserved data items $Y = \{y_1, y_2, \dots, y_N\}$, where $y_i \in \{1, 2, \dots, M\}$ whose values inform us the pixel comes from which gaussian distribution, then the likelihood function can be simplified significantly[4].

Assume the existence of joint density $p(X, Y; \Theta)$ and the data is independent identically distributed. Given $\Theta = \Theta^{i-1}$, then $L(\Theta)$ can be transformed as

$$L(\Theta) = Q(\Theta; \Theta^{i-1}) - H(\Theta; \Theta^{i-1}), \quad (2)$$

where

$$\begin{aligned} Q(\Theta; \Theta^{i-1}) &= \sum_{i=1}^N \sum_{l=1}^M \ln(a_l p_l(x_i; \Theta_l)) p(l|x_i; \Theta^{i-1}), \\ H(\Theta; \Theta^{i-1}) &= \sum_{i=1}^N \sum_{l=1}^M \ln(p(l|x_i; \Theta)) p(l|x_i; \Theta^{i-1}). \end{aligned}$$

The derivation of (2) can be found in [22].

With the help of EM algorithm, the function can be optimized directly. Notice that $p(l|x_i)$ is the probability to measure how likely x_i belongs to cluster l , and this is what we want in a segmentation model. Furthermore, considering that if the number of gaussian equals to the amount of points, then this probability can be used to measure the similarity between the corresponding two points. In our model, we will use this key point and construct a similarity metric by functional itself.

3 The Proposed Method: Normalized Cut with Adaptive Similarity and Spatial Regularization

3.1 Statistical Methods

In this section, we shall propose normalized cut segmentation models with adaptive similarity and spatial regularization under variational framework. To obtain a similarity concerning energy, inspired by parameter estimation of GMM and the EM algorithm, we model the image by empirical distribution, which has the form of GMM and introduce a auxiliary variable which can measure the similarity between points, then formulate the process of parameters estimation as an alternating optimization. In our model, the similarity function can be determined by the cost functional itself, which can be updated with the iteration goes on. To sum up, combining the normalized cut and common spatial regularization, we establish the model, which integrates the advantages of variational regularization and spectral clustering.

3.1.1 Empirical distribution of Image.

Let Ω be a discrete set in \mathbb{R}^2 , $I : \Omega \rightarrow \{0, 1, 2, \dots, 255\}$ stands for the image. Assume that each of the intensity value $I(x)$ be a realization of the random variable \mathcal{I} , then $\{I(x), x \in \Omega\}$ are samples of \mathcal{I} , and the normalized histogram of $\{I(x)\}$ can be expressed as

$$p(z) = \frac{1}{|\Omega|} \sum_{y \in \Omega} \delta(z - I(y)),$$

where

$$\delta(x) = \begin{cases} 1, & x = 0, \\ 0, & x \neq 0. \end{cases}$$

Notice $\delta(x)$ is not smooth, we replace it with a gaussian function $\delta_h(x)$, since the limitation of δ_h is the Delta function in the sense of distribution, where

$$\delta_h(x) = \frac{1}{\sqrt{2\pi}h} e^{-\frac{x^2}{2h^2}}.$$

When h is small, then it can approximate $\delta(x)$ well.

The smooth approximation of frequency histogram would be

$$p(z) = \frac{1}{|\Omega|} \sum_{y \in \Omega} \frac{1}{\sqrt{2\pi}h} e^{-\frac{(z - I(y))^2}{2h^2}}. \quad (3)$$

Obviously, $p(z)$ is a gaussian mixture distribution parameterized by h , so we deal with it by EM process as mentioned earlier. Here we indeed take full use of the property of term $p(l|x_i)$ mentioned previously so as to obtain an adaptive similarity.

3.1.2 Adaptive Similarity Functional

Assume that $\{I(x), x \in \Omega\}$ are samples of \mathcal{I} with the density $p(z)$ given in (3), then the log-likelihood function

$$L(h) = \sum_{x \in \Omega} \ln \frac{1}{|\Omega|} \sum_{y \in \Omega} \frac{1}{\sqrt{2\pi}h} e^{-\frac{(I(x) - I(y))^2}{2h^2}}.$$

Let us introduce a hidden random variable \mathcal{Y} , whose value y indicates the sample I comes from the y -th component of the gaussian mixtures. Then we have the complete data as $(\mathcal{I}, \mathcal{Y})$, in which $\mathcal{Y} = y$ means the sample I is produced by the y -th gaussian distribution. Here the number of gaussian component is $|\Omega|$, i.e. $y \in \{1, 2, \dots, |\Omega|\}$, then we have

$$L(h) = Q(h; h^{i-1}) - H(h; h^{i-1}), \quad (4)$$

where

$$Q(h; h^{i-1}) = \sum_{x \in \Omega} \sum_{y \in \Omega} \ln \left(\frac{1}{|\Omega|} p_y(I(x); h) p(y|I(x); h^{i-1}) \right),$$

and

$$H(h; h^{i-1}) = \sum_{x \in \Omega} \sum_{y \in \Omega} \ln p(y|I(x); h) p(y|I(x); h^{i-1}),$$

For the completeness of the paper, we list the details of derivation of (4) in Appendix A.

Using the fact

$$p_y(I(x); h) = \frac{1}{\sqrt{2\pi}h} e^{-\frac{(I(x)-I(y))^2}{2h^2}},$$

we plug it into Q , and then

$$Q(h; h^{i-1}) = \sum_{x \in \Omega} \sum_{y \in \Omega} \ln \left(\frac{e^{-(I(x)-I(y))^2/(2h^2)}}{\sqrt{2\pi}h|\Omega|} \right) p(y|I(x); h^{i-1}),$$

where $\sum_{y \in \Omega} p(y|I(x); h^{i-1}) = 1$.

Here $p(y|I(x); h)$ can be used to measure the similarity between $I(x)$ and $I(y)$. For these reason, we introduce an auxiliary variable $w : \Omega \times \Omega \rightarrow \mathbb{R}$, $w(x, y) = p(y|I(x); h)$, then the parameters estimation (4) can be converted to a minimization process

$$\min_{h \in \mathbb{H}, w \in \mathbb{C}_1} \left\{ E(h, w) = \sum_{x \in \Omega} \sum_{y \in \Omega} \left(\frac{(I(x)-I(y))^2}{2h^2} \right) w(x, y) + \sum_{x \in \Omega} \sum_{y \in \Omega} \ln(\sqrt{2\pi}h|\Omega|) w(x, y) + \sum_{x \in \Omega} \sum_{y \in \Omega} w(x, y) \ln w(x, y) \right\} \quad (5)$$

where $\mathbb{C}_1 = \{w : \Omega \times \Omega \rightarrow \mathbb{R} | 0 \leq w(x, y) \leq 1, \sum_{y \in \Omega} w(x, y) = 1, \forall x \in \Omega, \forall y \in \Omega\}$, $h \in \mathbb{H} = \{h : 0 < h_{min} \leq h \leq h_{max} < +\infty\}$.

The minimization problem (5) can be efficiently solved by the alternating scheme

$$\begin{cases} h^i = \arg \min_{h \in \mathbb{H}} E(h, w^{i-1}), \\ w^i = \arg \min_{w \in \mathbb{C}_1} E(h^i, w). \end{cases} \quad (6)$$

As for this iteration (6), our previous work [22] has proven the energy corresponding to this problem is decreasing with respect to the parameter h and it has

Lemma 1 (Likelihood Function Ascent [22]) *The sequence h^i produced by iteration (6) satisfies*

$$L(h^i) \geq L(h^{i-1}).$$

This lemma allows us to employ E to get a maximum likelihood estimator in which E is easier to be optimized than L .

Using Lagrangian multiplier method, we can easily get the closed-form solution of $w(x, y)$

$$w(x, y) = \frac{1}{S(x)} e^{-\frac{(I(x)-I(y))^2}{2h^2}}, \quad (7)$$

where $S(x) = \sum_{y \in \Omega} e^{-\frac{(I(x)-I(y))^2}{2h^2}}$ serves as a normalization factor. Obviously, $w(x, y)$ has the similar form of gaussian similarity function used in the full-connected graph [36], which can be used as a measure of similarity between image points. Since here the similarity is model-based, and it can be updated adaptively, which solve the problem of choosing parameters in similarity.

Since the existence of normalization factor $S(x)$ in the similarity function obtained by (7), the similarity w is asymmetric. In our model, we equip some symmetrization process to such a similarity. Here, we project the asymmetric similarity matrix to the convex set \mathbb{C}_2 which consists of symmetric matrix. For this projection, it is not difficult to get

Proposition 1 *Given set $\mathbb{C}_2 = \{A \in \mathbb{R}^{n \times n} | A = A^T\}$, then \mathbb{C}_2 is convex, and the projection of a matrix B onto \mathbb{C}_2 is $\frac{B+B^T}{2}$.*

To unify the normalized cut and the functional deduced by EM process, we add a projection process to our model, which serve as a symmetry matrix set constrain in the optimization process.

From EM process and the analysis of normalized cut, normalized cut functional and similarity functional are established, naturally, we propose the adaptive similarity normalized cut model with some spatial regularizers under variational framework.

3.2 Variational Framework

3.2.1 Some Definitions and Notations

Let $\Omega \subset \mathbb{R}^2$ be an open bounded set, and $I : \Omega \rightarrow \mathbb{R}$ be the image function. Meanwhile, $w : \Omega \times \Omega \rightarrow \mathbb{R}^+$ is a nonnegative smooth similarity function, $f : \Omega \rightarrow \mathbb{R}$ is bounded almost everywhere. Given $k_\epsilon : B_\epsilon \rightarrow \mathbb{R}^+$ is a smooth weighting function with $\int_{B_\epsilon} k_\epsilon(z) dz = 1$, where $B_\epsilon = \{z \in \mathbb{R}^2 : \|z\| < \epsilon\}$. Besides, let us denote the symbol “*” stand for a convolution operator, i.e. $(k_\epsilon * f)(x) = \int_{B_\epsilon} k_\epsilon(y) f(x - y) dy$.

3.2.2 Normalized Cut with Adaptive Similarity and Spatial Regularization

Based on the analysis in the previous sections, we propose the variational normalized cut model with adaptive similarity and spatial regularization as

$$\begin{aligned} \min_{w \in \mathbb{C}, f \in \mathbb{F}, h \in \mathbb{H}} & \left\{ \int_{\Omega \times \Omega} \left\{ \frac{(I(x) - I(y))^2}{2h^2} + \ln(\sqrt{2\pi}h|\Omega|) \right\} w(x, y) dx dy + \int_{\Omega \times \Omega} w(x, y) \ln w(x, y) dx dy \right. \\ & \left. + \lambda \int_{\Omega \times \Omega} w(x, y) ((k_\epsilon * f)(x) - (k_\epsilon * f)(y))^2 dx dy + \eta J(f) \right\}, \end{aligned} \quad (8)$$

where $\mathbb{C} = \{w \in L^\infty | 0 \leq w(x, y) \leq 1, \int_{\Omega} w(x, y) dy = 1, w(x, y) = w(y, x), a.e. x, y \in \Omega\}$, and $\mathbb{F} = \{f | |f(x)| < C, a.e. x \in \Omega, \int_{\Omega} f(x) d(x) dx = 0, \int_{\Omega} d(x) f^2(x) = 1, \forall x \in \Omega\}$, $\mathbb{H} = \{h : 0 < h_{min} \leq h \leq h_{max} < +\infty\}$, and λ, η are two positive parameters which can control the balance of each term in the cost functional.

Here we choose two popular regularizers in the field of computer vision: H^1 regularizer $J(f) = \int_{\Omega} \|\nabla f(x)\|^2 dx$ and TV regularizer $J(f) = \int_{\Omega} \|\nabla f(x)\| dx$. The normalized cut with adaptive similarity and H^1 regularization model, which is called NCASH¹ for short, can be optimized efficiently which is essentially a linear system. TV regularization model which is denoted by NCASTV for short, has superiority in segmentation which is verified in many models [7, 8, 32, 15], and can be solved by the operator splitting methods.

In fact, the first two terms serve as EM process, which endow the model adaptive similarity. More specifically, the first term can be seen as smoothness clustering criterion which is slight different the K-means’ piecewise constants version. Besides, there is a variance h to better discriminate pixels. The second term is a negative entropy regularizer, which force the similarity metric w to be smooth. The third term is the normalized cut energy, which serve as clustering and the last term formulates spatial regularization to make our segmentation results be smooth and robust to noise.

In the proposed methods, there are some convolution terms, which is beneficial to prove the existence of minimizers theoretically in a proper functional space [23], the convolution of a smooth kernel k_ϵ and f can be seen as a spatial regularization which will enhance the segmentation performance as well. Meanwhile, if we set ϵ small enough, then k_ϵ would be a delta function and the convolution operators would be disappeared.

3.2.3 Existence of Minimizer for the Proposed Models

In this section, we will theoretically prove the existence of minimizers for the proposed models. We will just give the result for NCASTV since both of NCASTV and NCASH¹ have minimizers by choosing proper function spaces (BV and H¹) and similar analysis method.

Let us consider the following energy functional for NCASTV model

$$E(f, w, h) = \int_{\Omega \times \Omega} \left\{ \frac{(I(x) - I(y))^2}{2h^2} + \ln(\sqrt{2\pi}h|\Omega|) \right\} w(x, y) dx dy + \int_{\Omega \times \Omega} w(x, y) \ln w(x, y) dx dy \\ + \lambda \int_{\Omega \times \Omega} w(x, y) ((k_\epsilon * f)(x) - (k_\epsilon * f)(y))^2 + \eta \int_{\Omega} \|\nabla f(x)\|^2 dx dy,$$

where $k_\epsilon : B_\epsilon \rightarrow \mathbb{R}$ is a polish function satisfying $\int_{B_\epsilon} K_\epsilon(z) dz = 1$. Without loss of generality, we assume $\lambda = 1$ and $\eta = 1$.

Here we will show the existence of one minimizer for NCASTV model in the following space

$$\mathbb{X} := \left\{ (f, w, h) : f \in BV(\Omega), w \in L^\infty(\Omega \times \Omega), 0 \leq w \leq 1, \int_{\Omega} f(x) dx = 0, \int_{\Omega} f^2(x) dx = 1, \right. \\ \left. \int_{\Omega} w(x, y) dy = 1, |f(x)| < C, w(x, y) = w(y, x), a.e. x \in \Omega, y \in \Omega, 0 < h_{min} \leq h \leq h_{max} < +\infty \right\}.$$

Theorem 1 *There exists at least one solution $(f^*, w^*, h^*) \in \mathbb{X}$ for NCASTV model, i.e.*

$$(f^*, w^*, h^*) = \arg \min_{(f, w, h) \in \mathbb{X}} E(f, w, h). \quad (9)$$

Proof: Details of the proof can be found in Appendix B.

4 Algorithms

4.1 Algorithm for NCASH¹ Model

The discrete algorithm of NCASH¹ model (8) can be directly minimized by alternating minimization algorithm, one may have the subproblems below

$$\left\{ \begin{array}{l} \min_{w \in \mathbb{C}_2} \max_{\beta} \left\{ \sum_{x \in \Omega} \sum_{y \in \Omega} \left\{ \frac{(I(x) - I(y))^2}{2h^2} + \ln(\sqrt{2\pi}h|\Omega|) \right\} w(x, y) + \sum_{x \in \Omega} \sum_{y \in \Omega} w(x, y) \ln w(x, y) \right. \\ \quad \left. + \sum_{x \in \Omega} \beta(x) \left(\sum_{y \in \Omega} w(x, y) - 1 \right) + \lambda \sum_{x \in \Omega} \sum_{y \in \Omega} w(x, y) ((k_\epsilon * f)(x) - (k_\epsilon * f)(y))^2 \right\}, \\ \min_{h \in \mathbb{H}} \left\{ \sum_{x \in \Omega} \sum_{y \in \Omega} \left\{ \frac{(I(x) - I(y))^2}{2h^2} + \ln(\sqrt{2\pi}h|\Omega|) \right\} w(x, y) \right\}, \\ \min_{f \in \mathbb{F}} \left\{ \lambda \sum_{x \in \Omega} \sum_{y \in \Omega} w(x, y) ((k_\epsilon * f)(x) - (k_\epsilon * f)(y))^2 + \eta \sum_{x \in \Omega} \|\nabla f(x)\|_2^2 \right\}, \end{array} \right.$$

where β is the lagrange multiplier, and λ, η are the parameters.

As for the w subproblem, we solve the corresponding optimization problem and then calculate the projection of w in \mathbb{C}_2 .

According to optimal condition, we have

$$\frac{(I(x) - I(y))^2}{2h^2} + 1 + \ln(\sqrt{2\pi}h|\Omega|) + \ln w(x, y) + \lambda((k_\epsilon * f)(x) - (k_\epsilon * f)(y))^2 + \beta(x) = 0.$$

Then

$$w(x, y) = e^{\frac{-(I(x) - I(y))^2}{h^2} - \lambda((k_\epsilon * f)(x) - (k_\epsilon * f)(y))^2} * A, \quad (10)$$

where

$$A = e^{-1 - \ln(\sqrt{2\pi}h|\Omega|) - \beta(x)}.$$

Since $\sum_{y \in \Omega} w(x, y) = 1$, we have

$$\frac{1}{A} = \sum_{y \in \Omega} e^{\frac{-(I(x) - I(y))^2}{h^2} - \lambda((k_\epsilon * f)(x) - (k_\epsilon * f)(y))^2}, \quad (11)$$

plug (11) into (10), then

$$w(x, y) = \frac{e^{\frac{-(I(x) - I(y))^2}{h^2} - \lambda((k_\epsilon * f)(x) - (k_\epsilon * f)(y))^2}}{\sum_{y \in \Omega} e^{\frac{-(I(x) - I(y))^2}{h^2} - \lambda((k_\epsilon * f)(x) - (k_\epsilon * f)(y))^2}}.$$

Since $w \in \mathbb{C}_2$, according to Proposition 1, the projection of similarity matrix W which consists of $w(x, y)$ is (the projection is also denoted as W)

$$W := \frac{W + W^T}{2}.$$

According to the optimal condition of h subproblem, then h can be optimized by

$$h^2 = Proj_{\mathbb{H}}\left(\frac{\sum_{x \in \Omega} \sum_{y \in \Omega} w(x, y)(I(x) - I(y))^2}{|\Omega|}\right).$$

Since

$$(K\mathbf{f})^T(D - W)K\mathbf{f} = \sum_{x \in \Omega} \sum_{y \in \Omega} w(x, y)((k_\epsilon * f)(x) - (k_\epsilon * f)(y))^2$$

where $K\mathbf{f}$ is the discretion of convolution $k_\epsilon * f$. Then f subproblem equals to a constrained linear problem

$$\min_{\substack{\mathbf{f}^T D \mathbf{f} = 1 \\ \mathbf{f}^T D \mathbf{1} = 0}} \lambda \mathbf{f}^T K^T (D - W) K \mathbf{f} + \eta \|\nabla \mathbf{f}\|_2^2, \quad (12)$$

where W is the similarity matrix, D is the degree matrix, and \mathbf{f} is the discretion of f .

Denote $\mathbf{z} = D^{\frac{1}{2}} \mathbf{f}$, the subproblem of \mathbf{f} can be converted to an eigenvalue type problem with respect to \mathbf{z} :

$$\min_{\substack{\|\mathbf{z}\|^2 = 1 \\ \mathbf{z}^T D^{\frac{1}{2}} \mathbf{1} = 0}} \mathbf{z}^T D^{-\frac{1}{2}} (\lambda K^T (D - W) K - \eta \Delta) D^{-\frac{1}{2}} \mathbf{z}.$$

This is a eigenvalue problem without the constraint $\mathbf{z}^T D^{\frac{1}{2}} \mathbf{1} = 0$. We can use Lagrangian method to address this constraint.

Define

$$\mathbb{S}_1 = \{\mathbf{z} : \|\mathbf{z}\|^2 = 1\}, \quad \mathbb{S}_2 = \{\mathbf{z} : \mathbf{z}^T D^{\frac{1}{2}} \mathbf{1} = 0\}.$$

Then by Lagrangian multiplier method, we have

$$\min_{\mathbf{z} \in \mathbb{S}_2} \min_{\mu} \left\{ \mathbf{z}^T D^{-\frac{1}{2}} (\lambda K^T (D - W) K - \eta \Delta) D^{-\frac{1}{2}} \mathbf{z} - \mu (\|\mathbf{z}\|^2 - 1) \right\}.$$

Please note here $-\mu$ is the standard Lagrangian multiplier and thus the above problem is a minimization problem with respect to μ . Otherwise, it should be a saddle problem with respect to \mathbf{z} and $-\mu$.

According to the first order optimal condition, we have

$$D^{-\frac{1}{2}}(\lambda K^T(D-W)K - \eta\Delta)D^{-\frac{1}{2}}\mathbf{z} - \mu\mathbf{z} = 0.$$

By projection gradient method, and inspired by Dinkelbach method [29] [14], we give the following iteration scheme

$$\begin{cases} \mu^k &= \frac{(\mathbf{z}^k)^T D^{-\frac{1}{2}}(\lambda K^T(D-W)K - \eta\Delta)D^{-\frac{1}{2}}\mathbf{z}^k}{(\mathbf{z}^k)^T \mathbf{z}^k}, \\ \hat{\mathbf{z}}^{k+1} &= \mathbf{z}^k - \tau(D^{-\frac{1}{2}}(\lambda K^T(D-W)K - \eta\Delta)D^{-\frac{1}{2}}\mathbf{z}^k - \mu^k \mathbf{z}^k), \\ \mathbf{z}^{k+1} &= Proj_{\mathbb{S}_2}(\hat{\mathbf{z}}^{k+1}). \end{cases} \quad (13)$$

In terms of the setting of μ^k , here we give a theorem to show that μ^k is decreasing as the iterations go on.

Theorem 2 Consider such an optimization problem

$$(P1) \quad \min_z \{\varphi^k(z) = \phi(z) - \mu(z^k)\psi(z)\}$$

where $\phi(z) = z^T P z$, $\psi(z) = z^T z$ and $\mu(z^k) = \frac{\phi(z^k)}{\psi(z^k)}$. If z^{k+1} solves (P1), then $\varphi^k(z^{k+1}) \leq 0$, $\mu(z^{k+1}) \leq \mu(z^k)$.

Proof: Since z^{k+1} solves (P1), then

$$\varphi^k(z^{k+1}) \leq \varphi^k(z^k) = \phi(z^k) - \mu(z^k)\psi(z^k). \quad (14)$$

For $\mu(z^k) = \frac{\phi(z^k)}{\psi(z^k)}$, (14) means $\varphi^k(z^{k+1}) \leq 0$, that is $\phi(z^{k+1}) - \mu(z^k)\psi(z^{k+1}) \leq 0$, simple transformation, then $\mu(z^{k+1}) \leq \mu(z^k)$.

If we set $P = D^{-\frac{1}{2}}(\lambda K^T(D-W)K - \eta\Delta)D^{-\frac{1}{2}}$, $\mu^k = \mu(\mathbf{z}^k)$, then we have μ^k in (13). Furthermore, since P is semi-positive, so $\{\mu^k\}$ is lower-bounded, which simply describes the convergence of $\{\mu^k\}$. Numerical experiments shown in Figure 4 demonstrate the convergence of μ^k .

Here, we pay more attention on the projection process

$$\mathbf{z}^{k+1} = Proj_{\mathbb{S}_2}(\hat{\mathbf{z}}^{k+1}),$$

which equals to the optimization of the lagrange function below

$$\min_{\mathbf{z}} \max_{\lambda} \frac{1}{2} \|\mathbf{z} - \hat{\mathbf{z}}^{k+1}\|^2 + \lambda \mathbf{z}^T D^{\frac{1}{2}} \mathbf{1},$$

where λ is the lagrange multiplier.

Then according to the optimal condition, we have

$$\mathbf{z}^{k+1} = \hat{\mathbf{z}}^{k+1} - \lambda D^{\frac{1}{2}} \mathbf{1}. \quad (15)$$

transposition of (15) and multiplied by $D^{\frac{1}{2}} \mathbf{1}$, then

$$\lambda = \frac{(\hat{\mathbf{z}}^{k+1})^T D^{\frac{1}{2}} \mathbf{1}}{\mathbf{1}^T D \mathbf{1}}, \quad (16)$$

plug (16) into (15), then

$$\mathbf{z}^{k+1} = Proj_{\mathbb{S}_2}(\hat{\mathbf{z}}^{k+1}) = \hat{\mathbf{z}}^{k+1} - \frac{(\hat{\mathbf{z}}^{k+1})^T D^{\frac{1}{2}} \mathbf{1}}{\mathbf{1}^T D \mathbf{1}} D^{\frac{1}{2}} \mathbf{1}.$$

To obtain the solution of (12), one can easily get

$$\mathbf{f} = D^{-\frac{1}{2}} \mathbf{z}$$

since D is diagonal and invertible.

To sum up, we give Algorithm 1 for NCASH¹ Model.

Algorithm 1 NCASH¹ Model

1. Given $\mathbf{f}^0 = \mathbf{1}$, $\mathbf{z}^0 = Proj_{\mathbb{S}_2}(\mathbf{f}^0)$, tolerant error = ϵ ; Set $\tau=2$, $h^0=50$, let $k = 0$.

2. Update similarity matrix

$$w^{k+1}(x, y) = \frac{e^{\frac{-(I(x)-I(y))^2}{2(h^k)^2} - \lambda(Kf^k(x) - Kf^k(y))^2}}{\sum_{y \in \Omega} e^{\frac{-(I(x)-I(y))^2}{2(h^k)^2} - \lambda(Kf^k(x) - Kf^k(y))^2}}.$$

3. Calculate the projection of W in \mathbb{C}_2

$$W^{k+1} = \frac{W^{k+1} + (W^{k+1})^T}{2}.$$

4. Update h

$$(h^{k+1})^2 = Proj_{\mathbb{H}}\left(\frac{\sum_{x \in \Omega} \sum_{y \in \Omega} w^{k+1}(x, y)(I(x) - I(y))^2}{|\Omega|}\right).$$

5. Calculate \mathbf{z}

$$\begin{cases} \mu^k &= \frac{(\mathbf{z}^k)^T D^{-\frac{1}{2}} (\lambda K^T (D - W^{k+1}) K - \eta \Delta) D^{-\frac{1}{2}} \mathbf{z}^k}{(\mathbf{z}^k)^T \mathbf{z}^k}, \\ \hat{\mathbf{z}}^{k+1} &= \mathbf{z}^k - \tau (D^{-\frac{1}{2}} (\lambda K^T (D - W^{k+1}) K - \eta \Delta) D^{-\frac{1}{2}} \mathbf{z}^k - \mu^k \mathbf{z}^k), \\ \mathbf{z}^{k+1} &= \hat{\mathbf{z}}^{k+1} - \frac{(\hat{\mathbf{z}}^{k+1})^T D^{\frac{1}{2}} \mathbf{1}}{\mathbf{1}^T D \mathbf{1}} D^{\frac{1}{2}} \mathbf{1}. \end{cases}$$

6. Reconstruct segmentation vector \mathbf{f}

$$\mathbf{f}^{k+1} = D^{-\frac{1}{2}} \mathbf{z}^{k+1}.$$

7. If $\frac{\|\mathbf{f}^{k+1} - \mathbf{f}^k\|^2}{\|\mathbf{f}^k\|^2} < \epsilon$, stop; Else, set $k = k + 1$, go to step 2.

4.2 Algorithm for NCASTV Model

The discrete algorithm of NCASTV model (8) also can be directly minimized by alternating minimization algorithm, one may have these subproblems

$$\left\{ \begin{array}{l} \min_{w \in \mathbb{C}_2} \max_{\beta} \left\{ \sum_{x \in \Omega} \sum_{y \in \Omega} \left\{ \frac{(I(x) - I(y))^2}{2h^2} + \ln(\sqrt{2\pi}h|\Omega|) \right\} w(x, y) + \sum_{x \in \Omega} \sum_{y \in \Omega} w(x, y) \ln w(x, y) \right. \\ \quad \left. + \sum_{x \in \Omega} \beta(x) \left(\sum_{y \in \Omega} w(x, y) - 1 \right) + \lambda \sum_{x \in \Omega} \sum_{y \in \Omega} w(x, y) ((k_\epsilon * f)(x) - (k_\epsilon * f)(y))^2 \right\}, \\ \min_{h \in \mathbb{H}} \left\{ \sum_{x \in \Omega} \sum_{y \in \Omega} \left\{ \frac{(I(x) - I(y))^2}{2h^2} + \ln(\sqrt{2\pi}h|\Omega|) \right\} w(x, y) \right\}, \\ \min_{f \in \mathbb{F}} \left\{ \lambda \sum_{x \in \Omega} \sum_{y \in \Omega} w(x, y) ((k_\epsilon * f)(x) - (k_\epsilon * f)(y))^2 + \eta \sum_{x \in \Omega} \|\nabla f(x)\|_2 \right\}, \end{array} \right.$$

where β is the lagrange multiplier, and λ, η are the parameters.

As for subproblem of w and h , we adopt the same process as NCASH¹ model. Here we mainly emphasis on subproblem of \mathbf{f}

$$\min_{\substack{\mathbf{f}^T D \mathbf{f} = 1 \\ \mathbf{f}^T D \mathbf{1} = 0}} \lambda \mathbf{f}^T K^T (D - W) K \mathbf{f} + \eta \|\nabla \mathbf{f}\|_2,$$

where W is the similarity matrix, D is the degree matrix, and \mathbf{f} is the discretization of f .

To solve \mathbf{f} subproblem, we adopt a splitting method, here we give the iteration scheme by penalty method. We introduce an auxiliary variable \mathbf{g} , which satisfies $\mathbf{g} = \mathbf{f}$, then we have the following problem

$$\min_{\substack{\mathbf{g}, \mathbf{f}^T D \mathbf{f} = 1 \\ \mathbf{f}^T D \mathbf{1} = 0}} \lambda \mathbf{f}^T K^T (D - W) K \mathbf{f} + \eta \|\nabla \mathbf{g}\|_2 + \epsilon \|\mathbf{f} - \mathbf{g}\|^2, \quad (17)$$

where ϵ is a penalty parameter.

Furthermore, we have two subproblems of problem (17)

$$\min_{\substack{\mathbf{f}^T D \mathbf{f} = 1 \\ \mathbf{f}^T D \mathbf{1} = 0}} \lambda \mathbf{f}^T K^T (D - W) K \mathbf{f} + \epsilon \|\mathbf{f} - \mathbf{g}\|^2, \quad (18a)$$

$$\min_{\mathbf{g}} \eta \|\nabla \mathbf{g}\|_2 + \epsilon \|\mathbf{f} - \mathbf{g}\|^2. \quad (18b)$$

As we can see, the (18b) problem is the ROF model for denoising, and (18a) problem is a linear problem which is similar to problem (12), so our model can be regarded as an alternating process of normalized cut and the denoising of the results of clustering. It is reasonable that our model will have a better performance. Since the ROF model can be efficiently solved [10, 8, 38], here we pay more attention on the problem (18a).

Here we make a transformation of \mathbf{f} , which is $\mathbf{z} = D^{-\frac{1}{2}} \mathbf{f}$. Therefore, the subproblem of \mathbf{f} can be converted to the problem concerning about \mathbf{z}

$$\min_{\substack{\|\mathbf{z}\|^2 = 1 \\ \mathbf{z}^T D^{\frac{1}{2}} \mathbf{1} = 0}} \mathbf{z}^T D^{-\frac{1}{2}} [\lambda K^T (D - W) K] D^{-\frac{1}{2}} \mathbf{z} + \epsilon \|D^{-\frac{1}{2}} \mathbf{z} - \mathbf{g}\|^2. \quad (19)$$

The same procedure as NCASH¹ model, we define

$$\mathbb{S}_1 = \{\mathbf{z} : \|\mathbf{z}\|^2 = 1\}, \quad \mathbb{S}_2 = \{\mathbf{z} : \mathbf{z}^T D^{\frac{1}{2}} \mathbf{1} = 0\}.$$

Adopting the projection gradient method, we calculate the optimal point in \mathbb{S}_1 by Lagrangian multiplier method, and then project the optimal point onto \mathbb{S}_2 .

The optimization problem (19) becomes

$$\min_{\mathbf{z} \in \mathbb{S}_2} \min_{\mu} \left\{ \mathbf{z}^T D^{-\frac{1}{2}} [\lambda K^T (D - W) K] D^{-\frac{1}{2}} \mathbf{z} + \epsilon \|D^{-\frac{1}{2}} \mathbf{z} - \mathbf{g}\|^2 - \mu (\|\mathbf{z}\|^2 - 1) \right\}.$$

To solve the above problem, by optimal condition of \mathbf{z} , we have

$$D^{-\frac{1}{2}} [\lambda K^T (D - W) K] D^{-\frac{1}{2}} \mathbf{z} + \epsilon (D^{-1} \mathbf{z} - D^{-\frac{1}{2}} \mathbf{g}) - \mu \mathbf{z} = 0. \quad (20)$$

As the same technique for NCASH¹, we get the Lagrangian multiplier

$$\mu = \frac{\mathbf{z}^T [\lambda D^{-\frac{1}{2}} K^T (D - W) K D^{-\frac{1}{2}} + \epsilon D^{-1}] \mathbf{z} - \epsilon \mathbf{z}^T D^{-\frac{1}{2}} \mathbf{g}}{\mathbf{z}^T \mathbf{z}}.$$

By projection gradient method, and following the previous method, we construct the iteration scheme:

$$\begin{cases} \mu^k &= \frac{(\mathbf{z}^k)^T D^{-\frac{1}{2}} [\lambda K^T (D - W) K + \epsilon I] D^{-\frac{1}{2}} \mathbf{z}^k - \epsilon \mathbf{z}^k D^{-\frac{1}{2}} \mathbf{g}}{(\mathbf{z}^k)^T \mathbf{z}^k}, \\ \hat{\mathbf{z}}^{k+1} &= \mathbf{z}^k - \tau (D^{-\frac{1}{2}} [\lambda K^T (D - W) K + \epsilon I] D^{-\frac{1}{2}} \mathbf{z}^k - \mu^k \mathbf{z}^k - \epsilon D^{-\frac{1}{2}} \mathbf{g}), \\ \mathbf{z}^{k+1} &= Proj_{\mathbb{S}_2}(\hat{\mathbf{z}}^{k+1}) = \hat{\mathbf{z}}^{k+1} - \frac{(\hat{\mathbf{z}}^{k+1})^T D^{\frac{1}{2}} \mathbf{1}}{\mathbf{1}^T D \mathbf{1}} D^{\frac{1}{2}} \mathbf{1}. \end{cases} \quad (21)$$

We also have a descent proposition for μ^k :

Theorem 3 Consider such an optimization problem

$$(P2) \quad \min_z \{ \varphi^k(z) = \phi(z) - \mu(z^k) \psi(z) \}$$

where $\phi(z) = z^T P z - z^T b$, $\psi(z) = z^T z$ and $\mu(z^k) = \frac{\phi(z^k)}{\psi(z^k)}$. If z^{k+1} solves (P2), then $\varphi^k(z^{k+1}) \leq 0$, $\mu(z^{k+1}) \leq \mu(z^k)$.

Proof: Similar to the proof of theorem 2.

Denote $P = D^{-\frac{1}{2}} (\lambda K^T (D - W) K + \epsilon I) D^{-\frac{1}{2}}$, $b = \epsilon D^{-\frac{1}{2}} \mathbf{g}$, $\mu^k = \mu(\mathbf{z}^k)$, then we have that μ^k in (21) satisfies theorem 3.

To recover \mathbf{f} , it can be easily done by

$$\mathbf{f} = D^{-\frac{1}{2}} \mathbf{z}$$

since D is invertible and diagonal.

We summary the algorithm for NCASTV in Algorithm 2 .

5 Experimental Results

Compared with traditional Ncut model, our proposed models have adaptive similarity and spatial regularization, so several experiments are designed to show the contributions of these two parts in this section. Then, we show some numerical results for the proposed methods and make comparisons with the most related methods. To simplify the computation, in the following experiments, we set k_ϵ be the delta function δ , thus $k_\epsilon * f = f$, which means $K = I$.

Algorithm 2 NCASTV Model

1. Given $\mathbf{f}^0 = \mathbf{z}^0 = \mathbf{g}^0 = \mathbf{1}$, tolerant error = ζ ; Set $\tau=2$, $h^0 = 50$. Let $k = 0$.

2. Update similarity matrix

$$w^{k+1}(x, y) = \frac{e^{\frac{-(I(x)-I(y))^2}{2h^{k2}} - \lambda(Kf^k(x)-Kf^k(y))^2}}{\sum_{y \in \Omega} e^{\frac{-(I(x)-I(y))^2}{2(h^k)^2} - \lambda(Kf^k(x)-Kf^k(y))^2}}.$$

3. Calculate the projection of W in \mathbb{C}_2

$$W^{k+1} = \frac{W^{k+1} + (W^{k+1})^T}{2}.$$

4. Calculate h

$$(h^{k+1})^2 = Proj_{\mathbb{H}}\left(\frac{\sum_{x \in \Omega} \sum_{y \in \Omega} w^{k+1}(x, y)(I(x) - I(y))^2}{|\Omega|}\right).$$

5. Calculate \mathbf{z}

$$\begin{cases} \mu^k = \frac{(\mathbf{z}^k)^T D^{-\frac{1}{2}} [\lambda K^T (D - W^{k+1}) K + \epsilon I] D^{-\frac{1}{2}} \mathbf{z}^k - \epsilon (\mathbf{z}^k)^T D^{-\frac{1}{2}} \mathbf{g}^k}{(\mathbf{z}^k)^T \mathbf{z}^k}, \\ \hat{\mathbf{z}}^{k+1} = \mathbf{z}^k - \tau (D^{-\frac{1}{2}} [\lambda K^T (D - W^{k+1}) K + \epsilon I] D^{-\frac{1}{2}} \mathbf{z}^k - \mu^k \mathbf{z}^k - \epsilon D^{-\frac{1}{2}} \mathbf{g}^k), \\ \mathbf{z}^{k+1} = \hat{\mathbf{z}}^{k+1} - \frac{(\hat{\mathbf{z}}^{k+1})^T D^{\frac{1}{2}} \mathbf{1}}{\mathbf{1}^T D \mathbf{1}} D^{\frac{1}{2}} \mathbf{1}. \end{cases}$$

6. Reconstruct \mathbf{f}

$$\mathbf{f}^{k+1} = D^{-\frac{1}{2}} \mathbf{z}^{k+1}.$$

7. Calculate the auxiliary variable

$$\mathbf{g}^{k+1} = ROF(\mathbf{f}^{k+1}, \frac{\eta}{2\epsilon}).$$

8. If $\frac{\|\mathbf{f}^{k+1} - \mathbf{f}^k\|^2}{\|\mathbf{f}^k\|^2} < \zeta$, stop; Or, set $k = k + 1$, return to step 3.

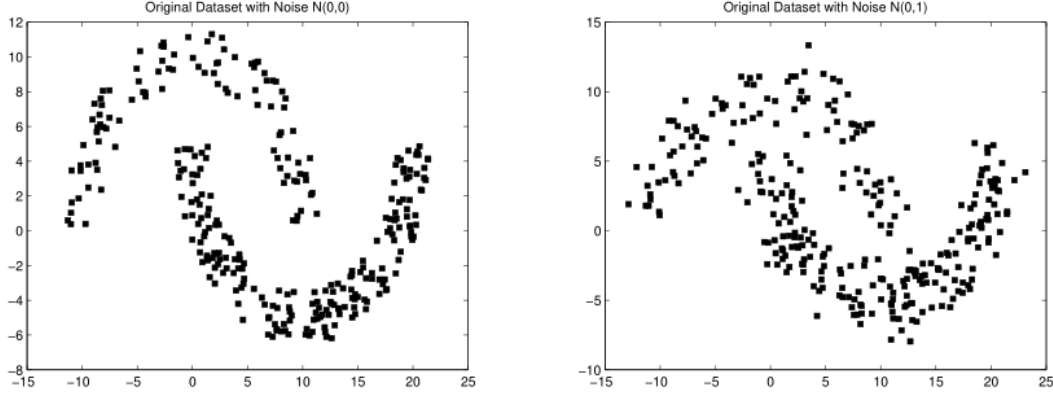


Figure 1: Double-moon data set and the data set corrupted by $N(0,1)$ are shown in the first and second figures, respectively.

5.1 Contribution of Regularization

The introduction of regularization makes our proposed models more robust under noise and better clustering or segmentation performance. To show the contribution of regularization in our proposed model, we have designed several experiments.

As to NCASH¹ model, we firstly give the results by the traditional Ncut model and proposed NCASH¹ model on the clean double-moon data set which consists of 300 points with two latent labels (Figure 1). And then we show the comparisons between these two methods on the noisy double-moon data set.

Without special statements, in the proposed NCASH¹ model, the parameters are set $\lambda = 1$, $\eta = 0.25 * \lambda$, and set h be a fixed value $h = 3$ to better show the effect of the regularizers. The similarity in Ncut is defined as the usually used $w(x, y) = e^{\frac{-(I(x)-I(y))^2}{h^2}}$, and similarity in NCASH¹ model is given in Algorithm 1.

In the first experiment (Figure 2), we show the clustering results for clean double-moon data set with Ncut and NCASH¹ models in the first column, the corresponding similarity matrices and the related eigenvectors are displayed in the last two columns. It is easy to find that both of the two methods can produce good clustering results. Analyzing these two eigenvectors, though Ncut produce oscillating eigenvector \mathbf{f} , it still can separate the data into two correct classes. Compare with Ncut method, the eigenvector \mathbf{f} provided by the proposed NCASH¹ is smoother. One can easily get two latent two classes according to the big jump point of eigenvector.

In the second experiment (Figure 3), let us see what will be happened when the double-moon data set contains gaussian noise with distribution $N(0,1)$. In this case, Ncut model produces undesirable results, which contains 24 wrong-labeled points. But our NCASH¹ model still can partition all the data points correctly due to the existence of regularizer. Since the adaptive similarity plays a fatal role on our model, here we show the similarity of Ncut model and NCASH¹ as well, one can find that both similarity produced by our method are block-diagonal, which is beneficial for a clustering process. This is the superiority of our model. However, under noise, the similarity of Ncut model is not so "clean", which means the existence of many abnormal data (the data with wrong label). As for the eigenvectors used for clustering, for the noisy data, the eigenvector by Ncut model has some serious oscillations and it fails to provide a good clustering criterion. Let us look at eigenvector by the proposed NCASH¹ model, it is still partible since there is a big jump in eigenvector and less oscillations in other points. This two experiments show that the proposed method is more robust fro noise than Ncut model.

Besides, as a numerical verification for theorem 2, we display the μ^k 's values during the iteration in Figure 4, which show that μ^k is converged.

As the NCASTV model for image segmentation, we show the segmentation results of sample

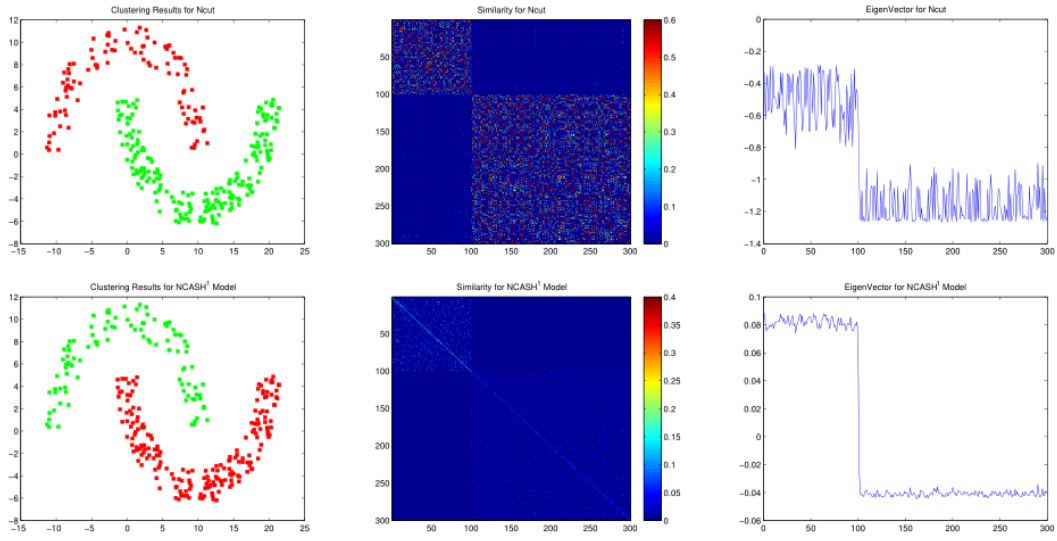


Figure 2: Results of Double-moon data set given by Ncut model and the proposed NCASH¹ model, and the corresponding similarity matrices and resulting eigenvectors.

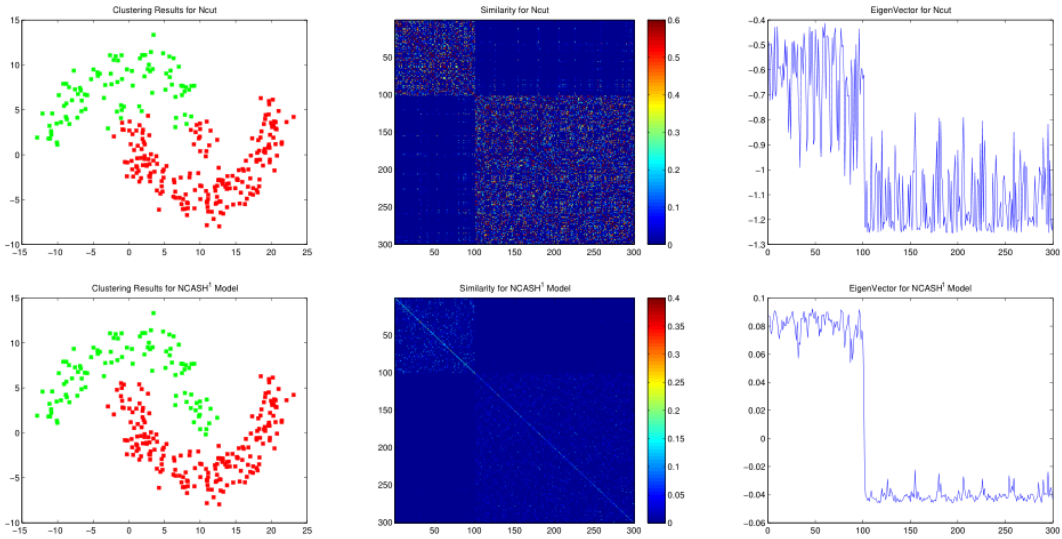


Figure 3: Results of Double-moon data set corrupted by $N(0,1)$ given by Ncut model and the proposed NCASH¹ model, and the corresponding similarity matrices and resulting eigenvectors.

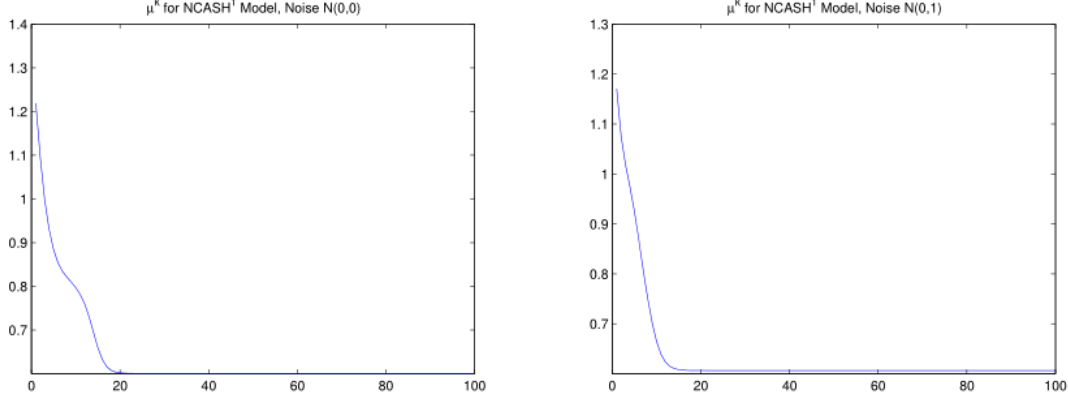


Figure 4: The values of μ^k appeared in NCASH¹ model on the clean data and noisy data, respectively.

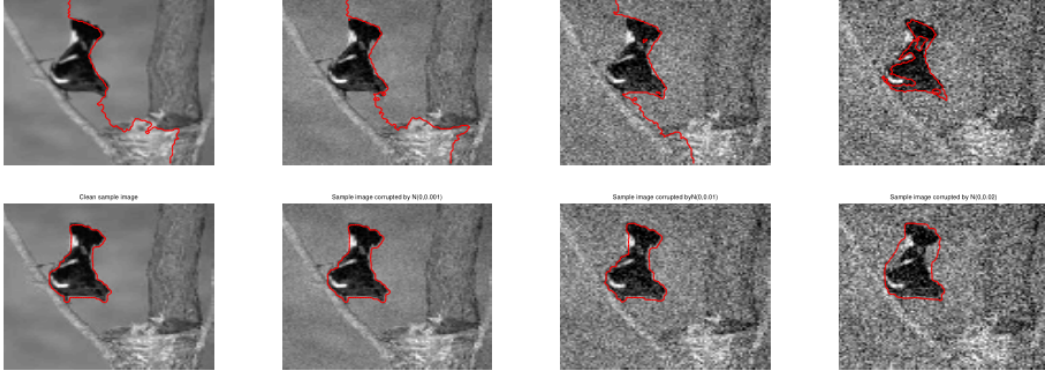


Figure 5: The segmentation results of sample image corrupted by $N(0,0)$, $N(0,0.001)$, $N(0,0.01)$, $N(0,0.02)$ given by Ncut model in the first row and by NCASTV model in the second row, with parameters in NCASTV model $\lambda = 1$, $\epsilon = 0.001 * \lambda$, and $\eta = 0.005 * \epsilon$, $\eta = 0.005 * \epsilon$, $\eta = 0.005 * \epsilon$, $\eta = 0.009 * \epsilon$, respectively.

image corrupted by gaussian noise with different level $N(0,0)$, $N(0,0.001)$, $N(0,0.01)$, $N(0,0.02)$, respectively in Figure 5. The sample images are all taken from BSDS500 database, and the parameters in NCASTV model are set as: $\lambda = 1$, $\epsilon = 0.001 * \lambda$, $\eta = 0.005 * \epsilon$ under noise $N(0,0)$, $N(0,0.001)$, $N(0,0.01)$, and $\eta = 0.009 * \epsilon$ under noise $N(0,0.02)$.

The experiments (Figure 5) show that our model is robust under noise with different variances, since spatial prior (TV regularization) plays a fatal role in our model. In the next experiment, we simply set the regularization parameter η different value: $0.001 * \epsilon$, $0.005 * \epsilon$, $0.01 * \epsilon$, and the other parameters are set: $\lambda = 1$, $\epsilon = 0.001 * \lambda$. The results in Figure 6 shows that with the regularization parameter becomes bigger and bigger, the segmentation results of the sample image (taken from BSDS500 database) become more smooth and the length of contour become shorter.

5.2 Contribution of Adaptive Similarity

To be contrasted with the traditional Ncut model, one of the key points in our proposed models is that the similarity in our model is determined by the energy functional itself and can be updated with the iteration goes on, which will greatly improve the results of segmentation. Since our proposed two models have the same similarity, here we pay attention to NCASTV model and demonstrate the contribution of similarity updating by showing the details of the



(a) NCASTV with $\eta = 0.001 * \epsilon$ (b) NCASTV with $\eta = 0.005 * \epsilon$ (c) NCASTV with $\eta = 0.01 * \epsilon$

Figure 6: The segmentation results of sample image by NCASTV model with different regularization parameters: $\eta = 0.001 * \epsilon$, $0.005 * \epsilon$, $0.01 * \epsilon$ respectively. The other parameters: $\lambda = 1$, $\epsilon = 0.001 * \lambda$.

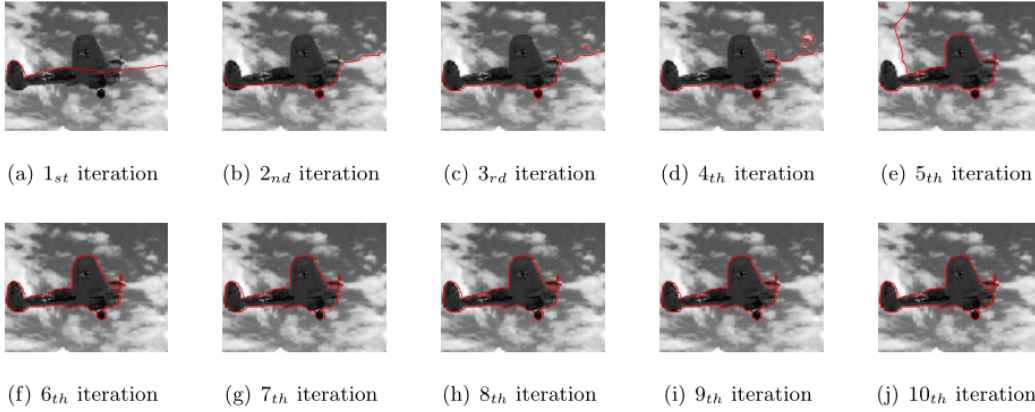


Figure 7: (a)-(j) show the first 10 iteration segmentation results of sample image by NCASTV model, with parameters $\lambda = 1$, $\epsilon = 0.001 * \lambda$, $\eta = 0.001 * \epsilon$.

iterations in the below experiments. Here we set the parameters in the NCASTV model: $\lambda = 1$, $\epsilon = 0.001 * \lambda$, $\eta = 0.001 * \epsilon$, and set the initial value of $h = 50$. The test image is taken from BSDS500 database [1], we show the first 10 iteration results by NCASTV model in (Figure 7).

From this experiment, one can find the segmentation results are greatly improved with the iteration goes on, since the similarity is adaptively updated by the model itself simultaneously. In fact, we deduce a better classification criterion than the traditional Ncut model [31].

5.3 Comparisons between Chan-Vese model, Pre-Ncut, NCASH¹ model and NCASTV model

Since there is no spatial prior information for the segmentation results by Ncut model, thus the segmentation results are always undesirable under noise. To improve the performance of Ncut model, a preprocessing is applied in Ncut [31]. [31] uses a kernel based filter to generate a edge-based image, and the similarity is calculated according to the edge-based image

$$w(x, y) = \begin{cases} e^{-\frac{(|(\nabla G * I)(x)|_2 - |(\nabla G * I)(y)|_2)^2}{2h^2}} & , x \neq y, \\ 1 & , x = y. \end{cases}$$

where G is the filter kernel. We call this algorithm as Pre-Ncut. In fact, Pre-Ncut is a edge based segmentation method and it is highly depended on the edge detector.

In the next experiments, we will give some comparisons between Chan-Vese model [7], Pre-Ncut [31] algorithm and proposed models. All the images used for testing algorithm are taken

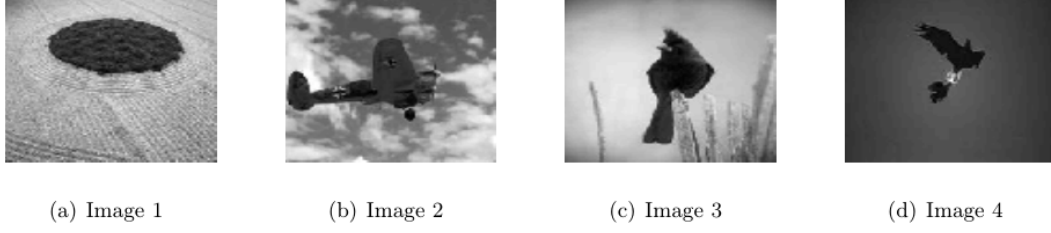


Figure 8: The sample images taken from BSDS500 database are resized to 100*100 for algorithm verification.

from BSDS500 database [1]¹. BSDS500 database is used for segmentation evaluation commonly, which consists of the original images and the corresponding ground-truth. There might be more than one ground-truth for one image given by different people. Since our proposed models are used for two phase segmentation, each of the ground-truth are merged artificially. Meanwhile, to test our method efficiently and save memory storage, we resize the original images and the corresponding ground-truth to the size of 100×100 , and set y only go through a 21×21 search window for every x . Here we choose four images from BSDS500 database which are denoted by Image1, Image2, Image3, Image4 (Figure 8) for convenience, and the results of these methods are shown in Figure 9. In these experiments, we set the parameters in NCASH¹ model: $\lambda = 1$, and $\eta = 0.001, 0.001, 0.0005, 0.001$ for different images, respectively, and parameters in NCASTV model: $\lambda = 1$, $\epsilon = 0.001 * \lambda$, and $\eta = 0.001 * \epsilon, 0.001 * \epsilon, 0.008 * \epsilon, 0.003 * \epsilon$ for different images, respectively.

Evaluation and Analysis

To evaluate the results taken from different method, here we consider two region quality criteria used for segmentation evaluation.

1.Variation of Information The Variation of Information [26] metric is used for clustering comparisons, which measures the distance between two clusterings with respect to their average conditional entropy given by

$$VI(S, S') = H(S) + H(S') - 2I(S, S'),$$

where H represents the entropy and I is the mutual information between two clusterings S and S' of data.

2.Rand Index The Rand Index [27] is designed for clustering evaluation, which measures the similarity between two data clusterings. The Rand Index between test segmentation S and the corresponding ground-truth segmentation G is defined as the sum of the amount of pixels pairs with same label in S and G and those with different labels in all segmentations, and then divided by the number of pixels pairs [1]. Given a test segmentation S and a set of corresponding ground-truth segmentations $\{G_k\}$, the Rand Index [34] [39] is given by

$$RI(S, \{G_k\}) = \frac{1}{T} \sum_{i < j} [c_{ij} p_{ij} + (1 - c_{ij})(1 - p_{ij})], \quad (22)$$

where event denoted by c_{ij} that pixels i and j with same label and the corresponding probability p_{ij} . T is the number of pairs of pixels. Here the p_{ij} was estimated by the sample mean, (22) means to average the Rand Index of all ground-truth segmentations.

With these region quality criteria, we give the VI values and RI values of four algorithms: Pre-Ncut, Chan-Vese, proposed NCASH¹ and NCASTV models in Table 1.

¹BSDS500 database: <https://www2.eecs.berkeley.edu/Research/Projects/CS/vision/grouping/resources.html>

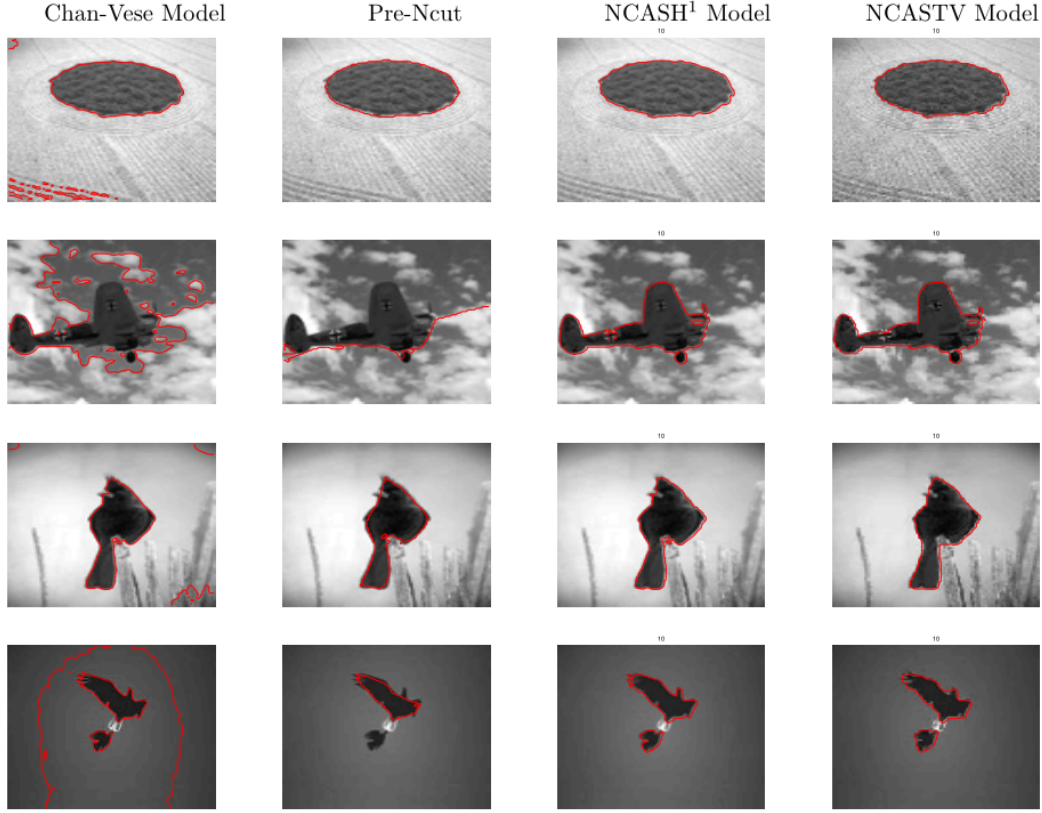


Figure 9: Comparison between Chan-Vese model, Pre-Ncut, NCASH¹ model and NCASTV model. Parameters in NCASH¹-based model: $\lambda = 1, \eta = 0.001 * \lambda, 0.001 * \lambda, 0.0005 * \lambda, 0.001 * \lambda$, respectively. Parameters in NCASTV model: $\lambda = 1, \epsilon = 0.001 * \lambda$, and $\eta = 0.001 * \epsilon, 0.001 * \epsilon, 0.008 * \epsilon, 0.003 * \epsilon$, respectively.

Table 1: Algorithms evaluation.

	Image 1		Image 2		Image 3		Image 4	
	VI	RI	VI	RI	VI	RI	VI	RI
Pre-Ncut	0.1268	0.9843	1.4567	0.5026	0.1760	0.9736	0.2010	0.9624
Chan-Vese	0.2710	0.9551	1.2914	0.5591	0.3811	0.9318	1.2053	0.5224
NCASH ¹	0.1219	0.9830	0.1986	0.9694	0.1311	0.9827	0.1018	0.9862
NCASTV	0.0793	0.9909	0.1930	0.9696	0.1853	0.9736	0.1378	0.9800

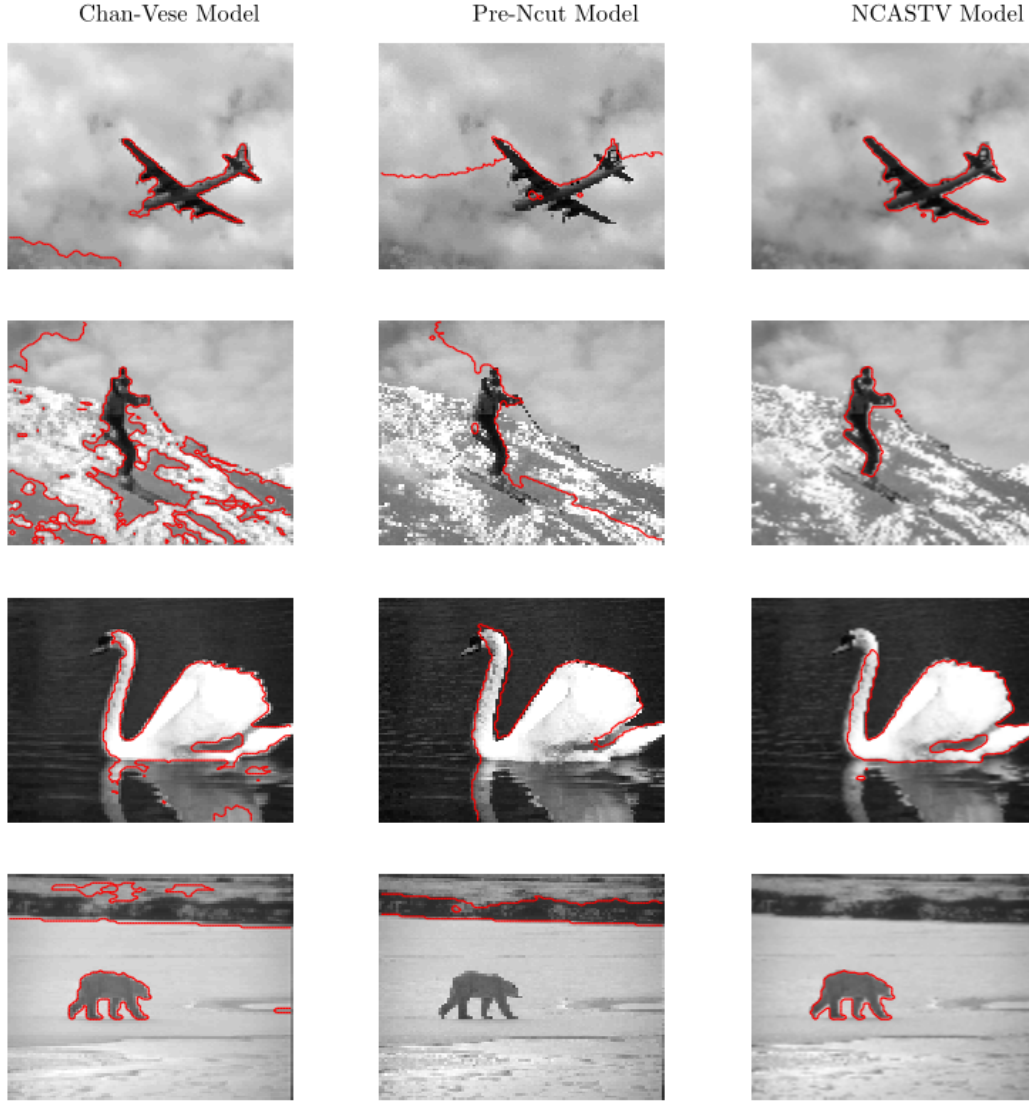


Figure 10: Comparison between Chan-Vese model, Pre-Ncut and NCASTV model, and parameters in NCASTV model all are: $\lambda = 1$, $\epsilon = 0.001 * \lambda$, and $\eta = 0.001 * \epsilon$.

The numerical results have shown visually that our proposed models have better performance than the traditional Pre-Ncut and classical K-means based Chan-Vese model, and the quantitative evaluation also demonstrates this point. From Table 1, one can find that the results of proposed models have smaller VI value and larger RI value, which means the results by proposed models are “closer” to the ground-truth segmentations and more similar to the ground-truth segmentations than the other methods. In fact, comparing our proposed model with the traditional Ncut model: firstly, the similarity of proposed model is determined by the model, so these model will behave more robust as for the setting of parameters. Secondly, our proposed models have regularization which will equip model with prior information to have better results. Compared with Chan-Vese model, the essential difference is that one is K-means based and another one is spectral clustering based. It is reasonable that the spectral clustering based methods usually have better performance.

In Figure 10, we give more comparison results for the Chan-Vese model, Pre-Ncut model and the proposed NCASTV model, the test images are taken from BSDS500 database, and parameters in NCASTV model all are: $\lambda = 1$, $\epsilon = 0.001 * \lambda$, and $\eta = 0.001 * \epsilon$.

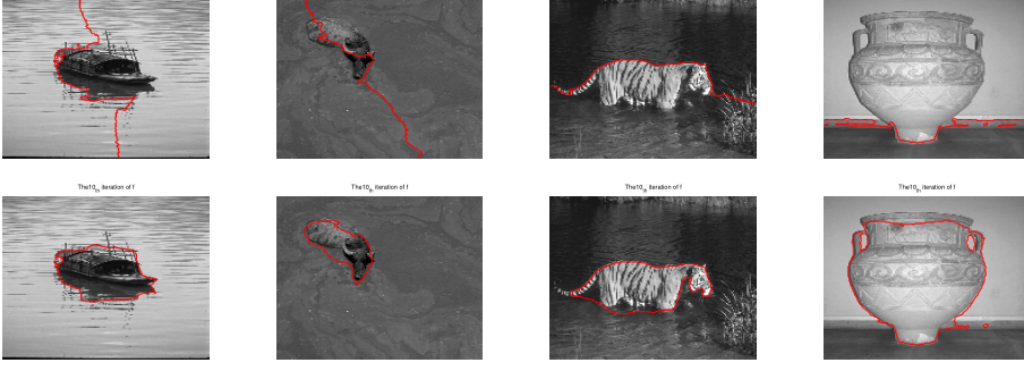


Figure 11: The comparison between Pre-Ncut and Pre-NCASTV model. The results by Pre-Ncut were shown in the first row, and the results by Pre-NCASTV model in the second row. The parameters in Pre-NCASTV model: $\lambda = 1$, $\epsilon = 0.001 * \lambda$, and $\eta = 0.03 * \epsilon, 0.005 * \epsilon, 0.02 * \epsilon, 0.05 * \epsilon$, respectively.

5.4 Pre-Ncut and Pre-NCASTV

Inspired by the skill used by preprocessing Ncut model, we equip some precondition process to our NCASTV model to establish a edge-based segmentation method, that is, the similarity in this method is adjusted to

$$w(x, y) = \begin{cases} \frac{e^{-\frac{(\|S(x)\|_2 - \|S(y)\|_2)^2}{2h^2} - \lambda(f(x) - f(y))^2}}{\sum_{y \in \Omega} e^{-\frac{(\|S(x)\|_2 - \|S(y)\|_2)^2}{2h^2} - \lambda(f(x) - f(y))^2}}, & x \neq y, \\ 1 & x = y. \end{cases}$$

where S is the edge-based image, and $S = (\nabla G * I)$.

In the experiments (Figure 11), we mainly make comparisons between Pre-Ncut and Pre-NCASTV, the images used for testing are also taken from BSDS500 database [1]. Here the size of image is $160 * 160$, and parameters in Pre-NCASTV model: $\lambda = 1$, $\epsilon = 0.001 * \lambda$, and $\eta = 0.03 * \epsilon, 0.005 * \epsilon, 0.02 * \epsilon, 0.05 * \epsilon$. One can find from these experiments, our proposed edge-based model have better performance. Further experiments and analysis of this model will delayed to our next work.

6 Conclusion

In this paper, we proposed a generalized nonlinear normalized cut model with adaptive similarity and spatial regularization. In our model, the similarity function which comes from EM process is not fixed but adaptively updated by the model itself and with the iteration of this similarity function goes on, the results of segmentation would be greatly improved. Moreover, we integrate the regularization technique in PDE into normalized cut under a variational framework, which enforce the segmentation boundaries to be spatially smooth and guarantee the robustness of the results under heavy noise.

Though the proposed methods have good performance, there are still some drawbacks. The time running the procedure is much longer than the traditional normalized cut model, since the existence of adaptive similarity updating. The NCASH¹ model and NCASTV model cost about 2 seconds and 3 seconds CPU time for 100×100 images for one outer iteration, respectively. In the future, the design of more efficient algorithm will be an interesting and attractive work.

A Derivation of equation (4)

Proof: For convenience, we denote $N = |\Omega|$, $\mathbf{z} \in \mathbb{R}^N$, $\mathbf{z} := \{I(x)|x \in \Omega\}$ and $\mathbf{c} \in \mathbb{R}^N$, $\mathbf{c} := \{y|y \in \Omega\}$.

It is easy to verified that

$$\begin{aligned} L(h) &= L(h) \sum_{\mathbf{c}} p(\mathbf{c}|\mathbf{z}; h^{i-1}) = \sum_{\mathbf{c}} \ln p(\mathbf{z}; h) p(\mathbf{c}|\mathbf{z}; h^{i-1}) \\ &= \sum_{\mathbf{c}} \ln p(\mathbf{z}, \mathbf{c}; h) p(\mathbf{c}|\mathbf{z}; h^{i-1}) - \sum_{\mathbf{c}} \ln p(\mathbf{c}|\mathbf{z}; h) p(\mathbf{c}|\mathbf{z}; h^{i-1}) \\ &\triangleq Q(h; h^{i-1}) - H(h; h^{i-1}), \end{aligned}$$

where $\mathbf{z} = \{z_1, z_2, \dots, z_N\}$, $\mathbf{c} = \{c_1, c_2, \dots, c_N\}$.

Under the i.i.d assumption of the data,

$$p(\mathbf{z}, \mathbf{c}; h) = \prod_{i=1}^N a_{c_i} p_{c_i}(z_i; h_{c_i}), \quad p(\mathbf{c}|\mathbf{z}; h^{i-1}) = \prod_{j=1}^N p(c_j|z_j; h^{i-1}).$$

Then

$$\begin{aligned} Q(h; h^{i-1}) &= \sum_{\mathbf{c}} \ln p(\mathbf{z}, \mathbf{c}; h) p(\mathbf{c}|\mathbf{z}; h^{i-1}) \\ &= \sum_{\mathbf{c}} \ln \left(\prod_{i=1}^N a_{c_i} p_{c_i}(z_i; h_{c_i}) \right) \prod_{j=1}^N p(c_j|z_j; h^{i-1}) \\ &= \sum_{\mathbf{c}} \sum_{i=1}^N \ln(a_{c_i} p_{c_i}(z_i; h_{c_i})) \prod_{j=1}^N p(c_j|z_j; h^{i-1}) \\ &= \sum_{c_1=1}^N \dots \sum_{c_N=1}^N \sum_{i=1}^N \ln(a_{c_i} p_{c_i}(z_i; h_{c_i})) \prod_{j=1}^N p(c_j|z_j; h^{i-1}) \\ &= \sum_{c_1=1}^N \dots \sum_{c_N=1}^N \sum_{i=1}^N \sum_{l=1}^N \delta_{l, c_i} \ln(a_l p_l(z_i; h_l)) \prod_{j=1}^N p(c_j|z_j; h^{i-1}) \\ &= \sum_{i=1}^N \sum_{l=1}^N \ln(a_l p_l(z_i; h_l)) \sum_{c_1=1}^N \dots \sum_{c_N=1}^N \delta_{l, c_i} \prod_{j=1}^N p(c_j|z_j; h^{i-1}). \end{aligned}$$

Notice that

$$\begin{aligned} &\sum_{c_1=1}^N \dots \sum_{c_N=1}^N \delta_{l, c_i} \prod_{j=1}^N p(c_j|z_j; h^{i-1}) \\ &= \sum_{c_1=1}^N \dots \sum_{c_{i-1}=1}^N \sum_{c_{i+1}=1}^N \dots \sum_{c_N=1}^N \sum_{c_i=1}^N \delta_{l, c_i} \prod_{j=1}^N p(c_j|z_j; h^{i-1}) \\ &= \sum_{c_1=1}^N \dots \sum_{c_{i-1}=1}^N \sum_{c_{i+1}=1}^N \dots \sum_{c_N=1}^N \prod_{j=1, j \neq i}^N p(c_j|z_j; h^{i-1}) p(l|z_i; h^{i-1}) \\ &= p(l|z_i; h^{i-1}) \sum_{c_1=1}^N p(c_1|z_1; h^{i-1}) \dots \sum_{c_{i-1}=1}^N p(c_{i-1}|z_{i-1}; h^{i-1}) \\ &\quad \sum_{c_{i+1}=1}^N p(c_{i+1}|z_{i+1}; h^{i-1}) \dots \sum_{c_N=1}^N p(c_N|z_N; h^{i-1}) \\ &= p(l|z_i; h^{i-1}) \prod_{j=1, j \neq i}^N \sum_{c_j=1}^N p(c_j|z_j; h^{i-1}) = p(l|z_i; h^{i-1}). \end{aligned}$$

Furthermore,

$$Q(h; h^{i-1}) = \sum_{i=1}^N \sum_{l=1}^N \ln(a_l p_l(z_i; h_l)) p(l|z_i; h^{i-1}).$$

Similarly,

$$H(h; h^{i-1}) = \sum_{i=1}^N \sum_{l=1}^N \ln(p(l|z_i; h)) p(l|z_i; h^{i-1}).$$

In fact, $L(h)$ has been transformed to the form below

$$\begin{aligned} L(h) &= Q(h; h^{i-1}) - H(h; h^{i-1}) \\ &= \sum_{i=1}^N \sum_{l=1}^N \ln(a_l p_l(z_i; h_l)) p(l|z_i; h^{i-1}) - \sum_{i=1}^N \sum_{l=1}^N \ln(p(l|z_i; h)) p(l|z_i; h^{i-1}). \end{aligned}$$

Since $a_l = \frac{1}{|\Omega|}$, we have

$$L(h) = \sum_{x \in \Omega} \sum_{y \in \Omega} \ln\left(\frac{1}{|\Omega|} p_y(I(x); h)\right) p(y|I(x); h^{i-1}) - \sum_{x \in \Omega} \sum_{y \in \Omega} \ln(p(y|I(x); h)) p(y|I(x); h^{i-1}).$$

B Proof of Theorem 1

$$\begin{aligned} J_1(w, h) &= \int_{\Omega \times \Omega} \left\{ \frac{(I(x) - I(y))^2}{2h^2} + \ln(\sqrt{2\pi}h|\Omega|) \right\} w(x, y) dx dy, \\ J_2(w) &= \int_{\Omega \times \Omega} w(x, y) \ln w(x, y) dx dy, \\ J_3(f, w) &= \int_{\Omega \times \Omega} [(k_\epsilon * f)(x) - (K_\epsilon * f)(y)]^2 w(x, y) dx dy, \\ J_4(f) &= \eta \int_{\Omega} \|\nabla f(x)\| dx. \end{aligned}$$

It is apparent that $J_3(f, w) \geq 0$, $J_4(f) \geq 0$. $J_1(w, h) \geq \ln(\sqrt{2\pi}|\Omega|h_{min})|\Omega|^2$. For any $t \geq 0$, $t \ln t \geq -\frac{1}{e}$, combining with the constraint of w , we can get $J_2(w) \geq -\frac{|\Omega|^2}{e}$. Therefore, $E(f, w, h)$ has a lower bound and $\inf_{(f, w, h) \in \mathbb{X}} E(f, w, h)$ exists. Denote $\{(f_n, w_n, h_n)\}$ be a minimizing sequence of problem (9), then

$$E(f_n, w_n, h_n) \rightarrow \inf_{(f, w, h) \in \mathbb{X}} E(f, w, h).$$

Since $\|w_n\|_{L^\infty(\Omega \times \Omega)} \leq 1$ and $w_n \in L^\infty(\Omega \times \Omega)$, $L^\infty(\Omega \times \Omega)$ is the conjugate of $L^1(\Omega \times \Omega)$ which is separable linear norm space, by the Banach-Alaoglu Theorem, there is a weak-* convergent subsequence which is also denoted as w_n and a weak-* limit $w \in L^\infty(\Omega \times \Omega)$ such that

$$w_n \rightharpoonup^* w \quad \text{in } L^\infty(\Omega \times \Omega),$$

That is, for any $\varphi \in L^1(\Omega \times \Omega)$,

$$\lim_{n \rightarrow +\infty} \int_{\Omega \times \Omega} w_n(x, y) \varphi(x, y) dx dy = \int_{\Omega \times \Omega} w(x, y) \varphi(x, y) dx dy.$$

since $w_n(x, y) \varphi(x, y) \leq \varphi(x, y)$ a.e. for any $\varphi > 0$, $\varphi \in L^1(\Omega \times \Omega)$. By Lebesgue dominated convergence theorem, we can get

$$\begin{aligned} \int_{\Omega \times \Omega} \lim_{n \rightarrow +\infty} w_n(x, y) \varphi(x, y) dx dy &= \int_{\Omega \times \Omega} w(x, y) \varphi(x, y) dx dy, \\ \int_{\Omega \times \Omega} \lim_{n \rightarrow +\infty} w_n(y, x) \varphi(x, y) dx dy &= \int_{\Omega \times \Omega} w(y, x) \varphi(x, y) dx dy, \end{aligned}$$

So $\int_{\Omega} \int_{\Omega} [w(x, y) - \lim_{n \rightarrow +\infty} w_n(x, y)] \varphi(x, y) dx dy = 0$ and $\int_{\Omega} \int_{\Omega} [w(x, y) - w(y, x)] \varphi(x, y) dx dy = 0$ hold for any $\varphi \in L^1(\Omega \times \Omega)$. Furthermore, $w(x, y) = \lim_{n \rightarrow +\infty} w_n(x, y)$ a.e. and $w(x, y) =$

$w(y, x)$ a.e. $x \in \Omega$ It's easy to verify that $0 \leq w(x, y) \leq 1$ a.e. $x \in \Omega$ and $\int_{\Omega} w(x, y) dy = 1$ a.e. $x \in \Omega$.

Especially, choose $\varphi(x, y) = \frac{(I(x)-I(y))^2}{2}$, we can get

$$\lim_{n \rightarrow +\infty} \int_{\Omega \times \Omega} \left\{ \frac{(I(x) - I(y))^2}{2} \right\} w_n(x, y) dx dy = \int_{\Omega \times \Omega} \left\{ \frac{(I(x) - I(y))^2}{2} \right\} w(x, y) dx dy.$$

By the constraint of h , $\{h_n\}$ is bounded in \mathbb{R} , so there exists a subsequence (which we relabel by n) such that $\lim_{n \rightarrow +\infty} h_n = h$. Combining with the fact that $\frac{1}{h^2}$ is a continuous with respect to h , we can get

$$\lim_{n \rightarrow +\infty} \frac{1}{h_n^2} = \frac{1}{h^2}.$$

Denote $J_1^{(1)}(w, h) = \int_{\Omega} \int_{\Omega} \left\{ \frac{(I(x)-I(y))^2}{2h^2} \right\} w(x, y) dx dy$, then

$$\begin{aligned} & |J_1^{(1)}(w_n, h_n) - J_1^{(1)}(w, h)| = |(J_1^{(1)}(w_n, h_n) - J_1^{(1)}(w, h_n)) + (J_1^{(1)}(w, h_n) - J_1^{(1)}(w, h))| \\ & \leq h_{max} \left| \int_{\Omega \times \Omega} \frac{(I(x) - I(y))^2}{2} (w_n(x, y) - w(x, y)) dx dy \right| + \|I\|_{L^\infty(\Omega)}^2 |\Omega|^2 \left| \frac{1}{h_n^2} - \frac{1}{h^2} \right|. \end{aligned}$$

While $n \rightarrow +\infty$, the right side of the above inequality is 0. Hence $\lim_{n \rightarrow +\infty} J_1^{(1)}(w_n, h_n) = J_1^{(1)}(w, h)$. Denote $J_1^{(2)}(w, h) = \ln(\sqrt{2\pi}h|\Omega|) \int_{\Omega} \int_{\Omega} w(x, y) dx dy$, then $J_1(w, h) = J_1^{(1)}(w, h) + J_1^{(2)}(w, h)$. Since $\ln(\sqrt{2\pi}h|\Omega|)$ is continuous with respect to h , then $\lim_{n \rightarrow +\infty} \ln(\sqrt{2\pi}h_n|\Omega|) = \ln(\sqrt{2\pi}h|\Omega|)$. Using the method as analysing $J_1^{(1)}(w, h)$, then we can get $\lim_{n \rightarrow +\infty} J_1^{(2)}(w_n, h_n) = J_1^{(2)}(w, h)$. Therefore

$$\lim_{n \rightarrow +\infty} J_1(w_n, h_n) = J_1(w, h).$$

Since $w \ln w$ is a continuous and convex function, $J_2(w)$ is weak-* lower semi-continuous with respect to w , i.e.

$$\lim_{n \rightarrow +\infty} \int_{\Omega \times \Omega} w_n(x, y) \ln w_n(x, y) dx dy \geq \int_{\Omega \times \Omega} w(x, y) \ln w(x, y) dx dy,$$

which indicates that $J_2(w_n) \geq J_2(w)$.

Now, we consider the convergence of $J_3(f_n, w_n)$.

Define $b_n(x, y) := [(k_\epsilon * f_n)(x) - (K_\epsilon * f_n)(y)]^2$, it is clear that $\{b_n(x, y)\}$ is uniformly bounded. Next we will consider the uniform boundedness of the sequence $\{\frac{\partial b_n}{\partial x}(x, y)\}$ and $\{\frac{\partial b_n}{\partial y}(x, y)\}$. Since

$$\frac{\partial b_n}{\partial x}(x, y) = 2[(K_\epsilon * f_n)(x) - (K_\epsilon * f_n)(y)] \left[\frac{\partial K_\epsilon}{\partial x} * f_n(x) \right],$$

$$\frac{\partial b_n}{\partial y}(x, y) = -2[(K_\epsilon * f_n)(x) - (K_\epsilon * f_n)(y)] \left[\frac{\partial K_\epsilon}{\partial y} * f_n(y) \right],$$

by Young inequality, we can immediately get that $\{b_n(x, y)\}$ is a bounded sequence in $W^{1,1}(\Omega \times \Omega)$. By Rellich-Kondrachov Compactness Theorem, there exists a subsequence of $\{b_n(x, y)\}$ (also denoted as b_n) and $b \in L^1(\Omega \times \Omega)$ such that $b_n(x, y) \rightarrow b(x, y)$ in $L^1(\Omega \times \Omega)$ strong.

$J_3(f, w)$ is a continuous and convex function with variable f , then it is weakly lower semi-continuous, i.e.

$$\lim_{n \rightarrow +\infty} \int_{\Omega \times \Omega} b_n(x, y) w(x, y) dx dy \geq \int_{\Omega \times \Omega} ((k_\epsilon * f)(x) - (K_\epsilon * f)(y))^2 w(x, y) dx dy.$$

Furthermore, owing to $w_n \rightharpoonup^* w$ in $L^\infty(\Omega \times \Omega)$, $b_n \rightarrow b$ in $L^1(\Omega \times \Omega)$, by some simple calculation, it is clear to get

$$\lim_{n \rightarrow +\infty} \int_{\Omega \times \Omega} b_n(x, y)[w_n(x, y) - w(x, y)]dxdy = 0.$$

Note that

$$J_3(f_n, w_n) = \int_{\Omega \times \Omega} b_n(x, y)w_n(x, y)dxdy = \int_{\Omega \times \Omega} b_n(x, y)[w_n(x, y) - w(x, y)]dxdy + \int_{\Omega \times \Omega} b_n(x, y)w(x, y)dxdy,$$

so we have

$$\liminf_{n \rightarrow +\infty} J_3(f_n, w_n) \geq J_3(f, w).$$

By the definition of $\{(f_n, w_n, h_n)\}$, the sequence $E(f_n, w_n, h_n)$ is bounded, i.e. there exists a constant M such that $J_1(w_n, h_n) + J_2(w_n) + J_3(f_n, w_n) + J_4(f_n) \leq M$. Since $J_1(w_n, h_n)$, $J_2(w_n)$, $J_3(f_n, w_n)$ are lower bounded, we can get $J(f_n)$ is upper bounded. Therefore the sequence $\{f_n\}$ is bounded in $BV(\Omega)$ and there exists a subsequence of $\{f_n\}$ (also denoted as f_n) and f in $BV(\Omega)$ such that $f_n \rightarrow f$ in $BV - weak^*$ and $f_n \rightarrow f$ in $L^1(\Omega)$ -strong, i.e.

$$\lim_{n \rightarrow +\infty} \int_{\Omega} f_n(x)dx = \int_{\Omega} f(x)dx, \quad \liminf_{n \rightarrow +\infty} J_4(f_n) \geq J_4(f).$$

It's obviously to get $\int_{\Omega} f(x)dx = 0$.

We can calculate

$$\begin{aligned} & \left| \int_{\Omega} f_n^2(x)dx - \int_{\Omega} f^2(x)dx \right| \\ & \leq \left| \int_{\Omega} f_n(x)(f_n(x) - f(x))dx \right| + \left| \int_{\Omega} f(x)(f_n(x) - f(x))dx \right| \\ & \leq \|f_n\|_{L^\infty(\Omega)} \left| \int_{\Omega} (f_n(x) - f(x))dx \right| + \|f\|_{L^\infty(\Omega)} \left| \int_{\Omega} (f(x) - f_n(x))dx \right| \\ & \leq C \left| \int_{\Omega} (f_n(x) - f(x))dx \right| + \|f\|_{L^\infty(\Omega)} \left| \int_{\Omega} (f(x) - f_n(x))dx \right|. \end{aligned}$$

Let $n \rightarrow +\infty$, we can get

$$\lim_{n \rightarrow +\infty} \left| \int_{\Omega} f_n^2(x)dx - \int_{\Omega} f^2(x)dx \right| \leq 0.$$

So we can get

$$\int_{\Omega} f^2(x)dx = \lim_{n \rightarrow +\infty} \int_{\Omega} f_n^2(x)dx = 1.$$

Hence, $(f, w, h) \in \mathbb{X}$ is a solution of NCASTV model, which completes our proof.

References

- [1] P. Arbelaez, M. Maire, C. C. Fowlkes, et al(2011), *Contour detection and hierarchical image segmentation*, IEEE Transactions on Pattern Analysis and Machine Intelligence, 33(5), pp. 898-916.
- [2] J. Ashburner, K. J. Friston(2005), *Unified segmentation*. Neuroimage, 26(3), pp. 839-851.
- [3] M. Belkin, P. Niyogi(2003), *Laplacian eigenmaps for dimensionality reduction and data representation*, Neural computation, 15(6), pp. 1373-1396.

- [4] J. A. Bilmes(2000), *A gentle tutorial of the EM algorithm and its application to parameter estimation for gaussian mixture and hidden Markov models*, International Computer Science Institute, 4, pp. 2-7.
- [5] T. Buhler, M. Hein(2009), *Spectral clustering based on the graph p-laplacian*, International Conference on Machine Learning, pp. 81-88.
- [6] V. Caselles, F. Catte, T. Coll, et al(1993), *A geometric model for active contours in image processing*, Numerische Mathematik, 66(1), pp. 1-31.
- [7] T. F. Chan, L. A. Vese(2001), *Active contours without edges*, IEEE Transactions on Image Processing, 10(2), pp. 266-277.
- [8] A. Chambolle(2004), *An algorithm for total variation minimization and applications*, Journal of Mathematical Imaging and Vision, 20(1), pp. 89-97.
- [9] F. R. K. Chung(1997), *Spectral Graph Theory*, Betascript Publishing.
- [10] T. F. Chan, G. H. Golub, P. Mulet, et al(1999), *A nonlinear primal-dual method for total variation-based image restoration*, SIAM Journal on Scientific Computing, 20(6), pp. 1964-1977.
- [11] G. Dong, M. Xie(2005), *Color clustering and learning for image segmentation based on neural networks*, IEEE Transactions on Neural Networks, 16(4), pp. 925-936.
- [12] A. P. Eriksson, C. Olsson, F. Kahl, et al(2007), *Normalized cuts revisited: A reformulation for segmentation with linear grouping constraints*, International Conference on Computer Vision, pp. 1-8.
- [13] C. Gao, D. Zhou, Y. Guo, et al(2013), *Automatic iterative algorithm for image segmentation using a modified pulse-coupled neural network*, Neurocomputing, pp. 332-338.
- [14] B. Ghanem, N. Ahuja(2010), *Dinkelbach NCUT: An efficient framework for solving normalized cuts problems with priors and convex constraints*, International Journal of Computer Vision, 89(1), pp. 40-55.
- [15] G. Gilboa, S. Osher(2008), *Nonlocal operators with applications to image processing*, Siam Journal on Multiscale Modeling and Simulation, 7(3), pp. 1005-1028.
- [16] T. Goldstein, S. Osher(2009), *The split bregman method for L1-regularized problems*, Siam Journal on Imaging Sciences, 2(2), pp. 323-343.
- [17] L. Gorelick, O. Veksler, Y. Boykov, et al(2014), *Convexity shape prior for segmentation*, European Conference on Computer Vision, pp. 675-690.
- [18] L. Hagen, A. B. Kahng(1992), *New spectral methods for ratio cut partitioning and clustering*, IEEE Transactions on Computer-Aided Design of Integrated Circuits and Systems, 11(9), pp. 1074-1085.
- [19] Z. Iscan, A. Yuksel, Z. Dokur, et al(2009), *Medical image segmentation with transform and moment based features and incremental supervised neural network*, Digital Signal Processing, 19(5), pp. 890-901.
- [20] A. K. Jain(2010), *Data clustering: 50 years beyond K-means*, International Conference on Pattern Recognition, 31(8), pp. 651-666.
- [21] M. Kass, A. Witkin, D. Terzopoulos, et al(1988), *Snakes: active contour models*, International Journal of Computer Vision, 1(4), pp. 321-331.

- [22] J. Liu, H. Zhang(2013), *Image segmentation using a local GMM in a variational framework*, Journal of Mathematical Imaging and Vision, 46(2), pp. 161-176.
- [23] J. Liu, X. Zheng(2017), *A block nonlocal TV method for image restoration*, Siam Journal on Imaging Sciences, 10(2), pp. 920-941.
- [24] Z. Liu, D. W. Jacobs, R. Basri(1999), *The role of convexity in perceptual completion: Beyond good continuation*, Vision Research, 39(25), pp. 4244-4257.
- [25] C. Li, C. Kao, J. C. Gore, et al(2008), *Minimization of region-scalable fitting energy for image segmentation*, IEEE Transactions on Image Processing, 17(10), pp. 1940-1949.
- [26] M. Meila(2005), *Comparing clusterings: An axiomatic view*, International Conference on Machine Learning, pp. 577-584.
- [27] W. M. Rand(1971), *Objective criteria for the evaluation of clustering methods*, Journal of the American Statistical Association, 66(336), pp. 846-850.
- [28] D. Reynolds(2015), *Gaussian mixture models*, Encyclopedia of biometrics, pp. 827-832.
- [29] R. G. Rodenas, M. Rodriguez, D. V. Rayo, et al(1999), *Extensions of Dinkelbach's algorithm for solving non-linear fractional programming problems*, Top, 7(1), pp. 33-70.
- [30] A. Sarkar, M. K. Biswas, B. Kartikeyan, et al(2002), *A MRF model-based segmentation approach to classification for multispectral imagery*, IEEE Transactions on Geoscience and Remote Sensing, 40(5), pp. 1102-1113.
- [31] J. Shi, J. Malik(2000), *Normalized cuts and image segmentation*, IEEE Transactions on Pattern Analysis and Machine Intelligence, 22(8), pp. 888-905.
- [32] A. Szlam, X. Bresson(2009), *A total variation-based graph clustering algorithm for cheeger ratio cuts*, UCLA Cam Report, pp. 09-68.
- [33] M. Tang, D. Marin, I. B. Ayed, et al(2016), *Normalized cut meets mrf*, European Conference on Computer Vision, pp. 748-765.
- [34] R. Unnikrishnan, C. Pantofaru, M. Hebert(2007), *Toward objective evaluation of image segmentation algorithms*, IEEE Transactions on Pattern Analysis and Machine Intelligence, 29(6), pp. 929-944.
- [35] O. Veksler(2008), *Star shape prior for graph-cut image segmentation*, European Conference on Computer Vision, pp. 454-467.
- [36] U. Von Luxburg(2007), *A tutorial on spectral clustering*, Statistics and Computing, 17(4), pp. 395-416.
- [37] Z. Wu, R. Leahy(1993), *An optimal graph theoretic approach to data clustering: Theory and its application to image segmentation*, IEEE Transactions on Pattern Analysis and Machine Intelligence, 15(11), pp. 1101-1113.
- [38] C. Wu, X. Tai(2010), *Augmented lagrangian method, dual methods, and split bregman iteration for ROF, vectorial TV, and high order models*, Siam Journal on Imaging Sciences, 3(3), pp. 300-339.
- [39] A. Y. Yang, J. Wright, Y. Ma, et al(2008), *Unsupervised segmentation of natural images via lossy data compression*, Computer Vision and Image Understanding, 110(2), pp. 212-225.

- [40] S. X. Yu, J. Shi(2004), *Segmentation given partial grouping constraints*, IEEE Transactions on Pattern Analysis and Machine Intelligence, 26(2), pp. 173-183.
- [41] Y. Yu, C. Fang, Z. Liao(2015), *Piecewise flat embedding for image segmentation*, IEEE International Conference on Computer Vision (ICCV) (2015), pp. 1368-1376.
- [42] H. Zhuang, K. S. Low, W. Yau, et al(2012), *Multichannel Pulse-Coupled-Neural-Network-Based Color Image Segmentation for Object Detection*, IEEE Transactions on Industrial Electronics, 59(8), pp. 3299-3308.